Simulations de CI optiques sous Opti-BPM

L. Bastard, D. Bucci

I - Environnement de travail

Sur les postes du LHOG :

- login = userlocal ; mot de passe = CIMEnano
- créer un répertoire personnel sur le serveur (raccourci sur le bureau), dans le répertoire BE_Optique_PG3A
- lancer le logiciel : optiBPM (raccourci sur le bureau)
- vous travaillerez en local, pour sauvegarder vos fichiers sur le serveur à la fin de chaque séance

II - Matériaux et guides

Lorsque l'on démarre le logiciel, il faut tout d'abord créer un nouveau projet avec la commande : File -> New. Une fenêtre apparaît alors pour permettre de fixer les paramètres principaux.

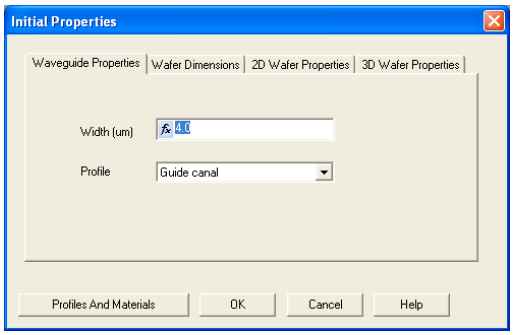

- Width = largeur par défaut des guides (laisser a 4 µm)
- Profile = structure d'indice des guides. Cette structure d'indice n'existe pas, il faut la créer => profiles and materials (lance le logiciel « profile designer »)

Profile designer : dans cette interface, on peut créer des matériaux et des structures guidantes. Ces paramètres sont enregistrés dans une arborescence. Par défaut il existe deux racines à cette arborescence : « master » et « optiBPM Designer1 ». On créera tous les matériaux et profiles dans « optiBPM Designer1 ».

- Créer 2 matériaux diélectriques : « verre » et « verre dopé » d'indices respectifs 1.5 et 1.51
- N'oubliez pas de sauvegarder chacun d'eux (store)
- Créer un nouveau guide canal : guidecanal1, de matériau « verre dopé » : il faut en effet préciser le matériau de haut indice comme matériau constituant le guide d'onde.
- Quitter le profile designer

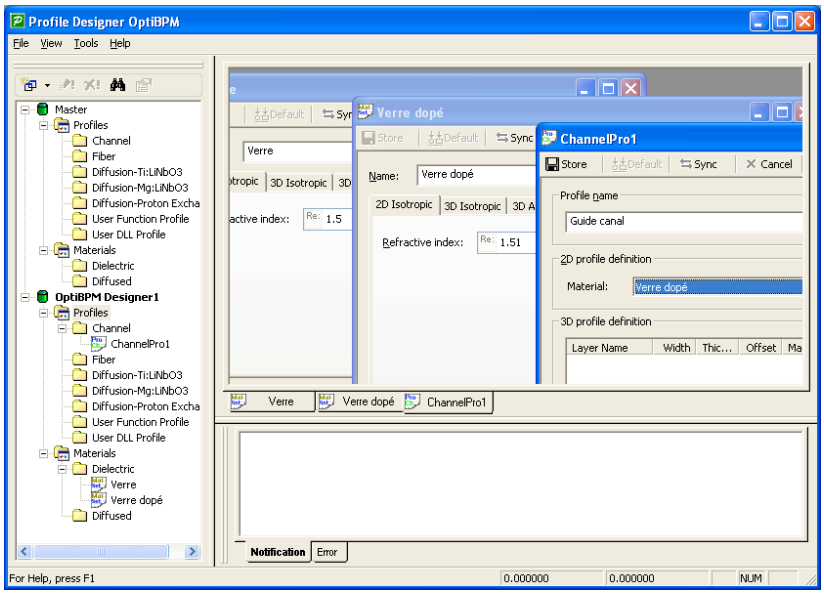

Dans **layout designer** :

- Mettre le profil d'indice que vous venez de créer (guidecanal1)
- Onglet wafer dimensions : laisser les valeurs par défaut
- Onglet 2D wafer properties et 3D wafer properties : entrer le matériau du substrat (verre)
- Ces paramètres peuvent être modifiés plus tard dans :
    - Edit -> wafer properties
    - Edit -> default waveguide
    - Edit -> profile and materials

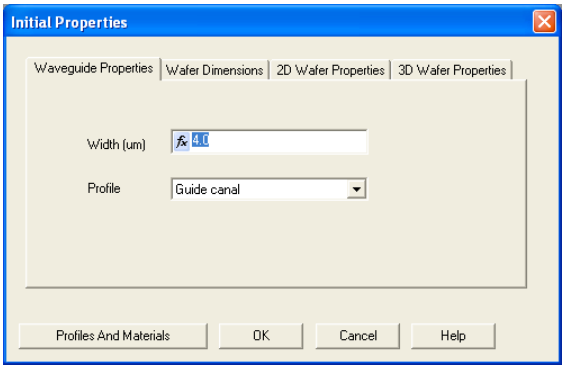

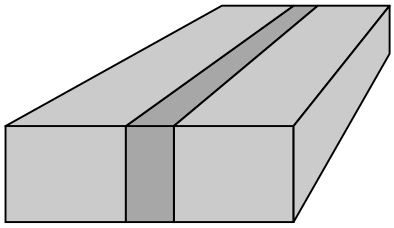

Profil d'indice d'un guide 2D

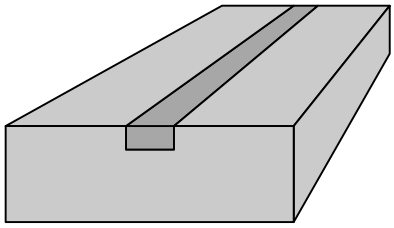

Profil d'indice d'un guide 3D

III - Un peu de dimensionnement

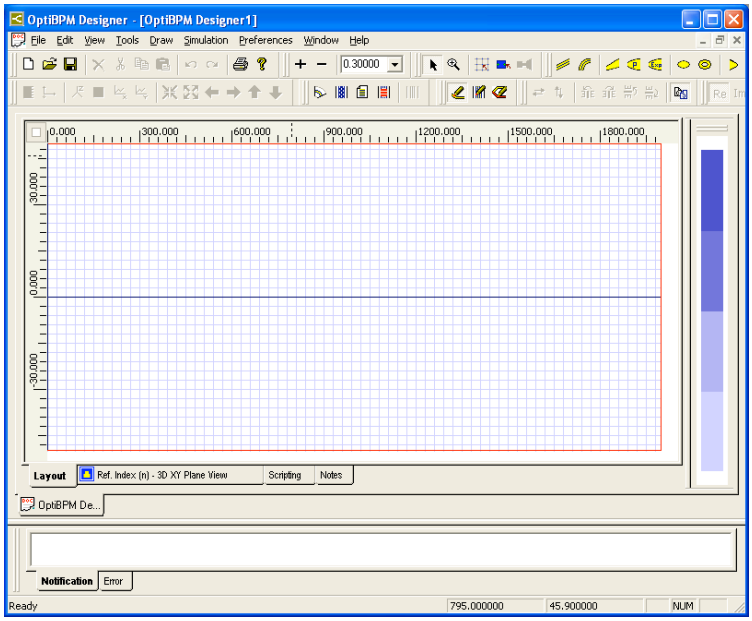

Note : si le logiciel n'a pas encore été configuré, il se peut que vous n'ayez pas accès à la totalité des barres d'outils. Si besoin est, vous pouvez déplacer les premières barres d'outil vers le bas de façon à les avoir toutes visibles.

Créer un guide droit (barre d'outils)

- Longueur = 1mm
- Largeur = 5 µm
- Centré en (0,0)
- Nom = guide1

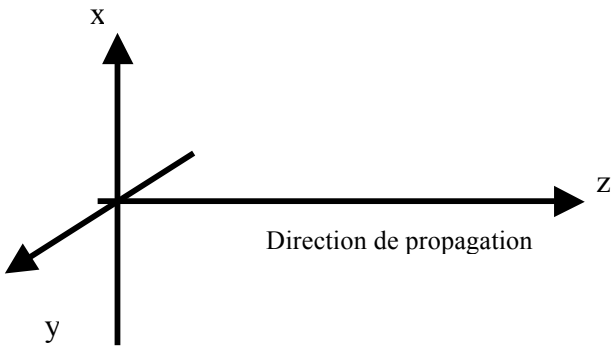

Note : la largeur des guides est un paramètre que l'on a souvent besoin de faire varier, nous allons créer une variable pour y accéder plus rapidement (cela devient très utile lorsqu'on a un dispositif avec beaucoup de guides !)

- Créer une variable dans Simulation -> Edit parameter -> User variable : nom = largeur, valeur = 5. On pourra ensuite faire varier la valeur de « largeur » dans un script (voir plus loin…)
- Sauvegarder
- Remplacer la largeur du guide par « largeur ».

IV - Simulation !

Créer un plan d'entrée (input plane). Le bouton se trouve dans la barre d'outil.

- Position : z=0
- Champ : rectangulaire

Dans l'onglet « Input field 2D » :

Une fois le plan d'entrée positionné, il faut définir quel champ optique est imposé au niveau de ce plan. Ce champ peut être soit centré sur un guide (auto), soit centré à un endroit sur le plan d'entrée défini par sa cote *x* (user)

- Edit
- Cocher le guide puis cliquer sur « Add <- » (ceci crée un champ centré sur le guide coché, donc « auto »)
- Régler la taille du champ a 3 µm avec « Edit »
- Valider avec OK

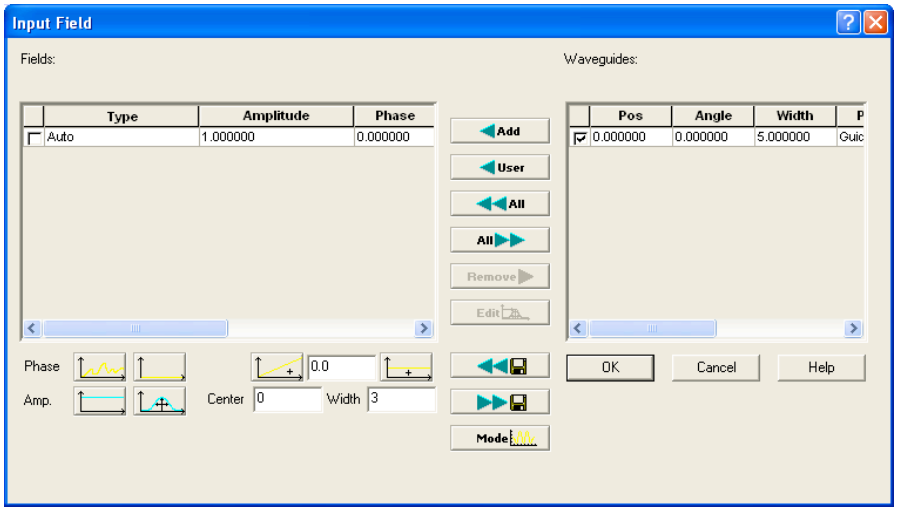

Pour lancer la simulation = propagation du champ d'entrée dans la structure

- Simulation -> Calculate 2D isotropic solution
- Ref. index : Average
- Longueur d'onde : 1,3 µm

Les résultats sont visualisés avec le programme « Result viewer »
Tester le couplage de la lumière dans le guide droit pour différents champs d'entrée :

- Gaussien de largeur 5 microns centré sur le guide puis décalé de 2 µm
- Modal (ici, le champ est forcément lié au guide : l'option de centrage est grisée et le champ est forcément « auto »)
- User : aller dans « calculate mode » pour calculer le champ d'ordre 1 puis le sauver et l'utiliser comme champ d'entrée.

V - Mesures

Il est souvent intéressant de faire des mesures pour évaluer un dimensionnement. Celles-ci sont disponibles dans Simulation -> Additional output data

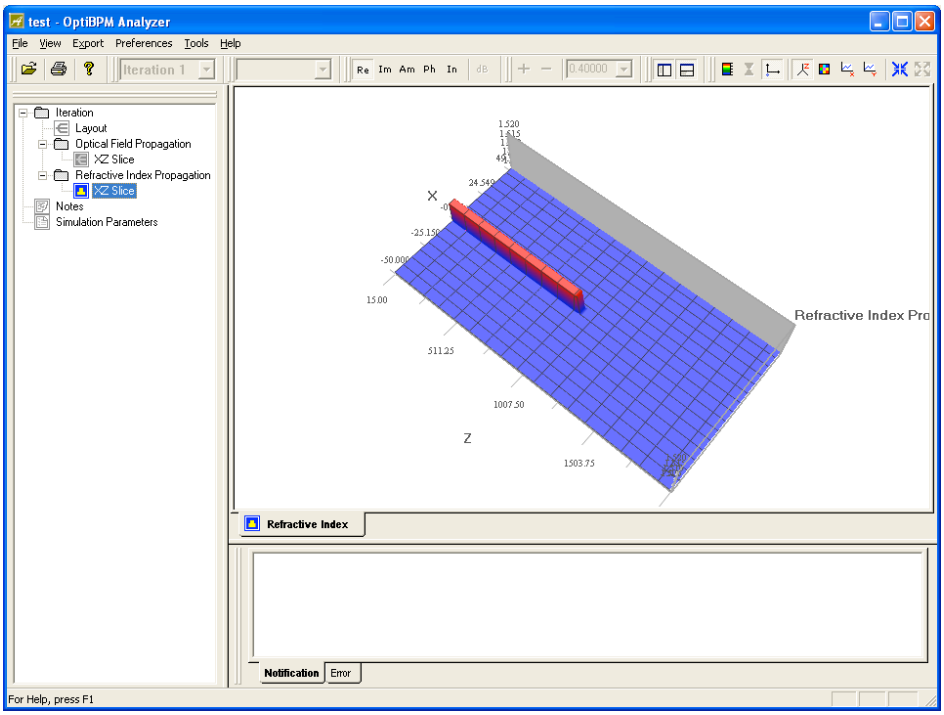

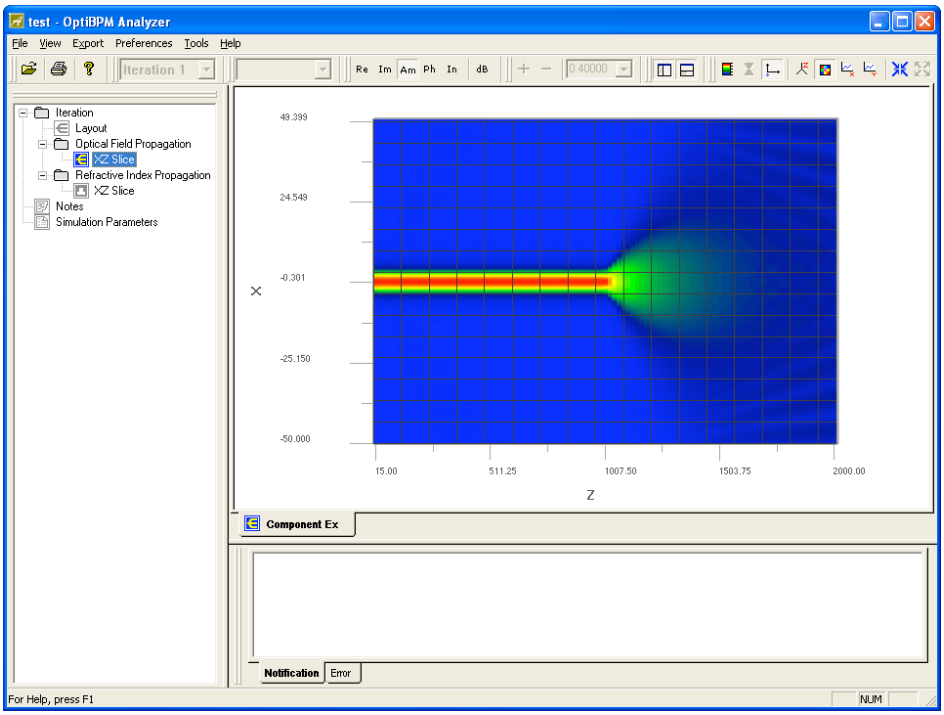

- Relative power : puissance totale dans la fenêtre de calcul en fonction de la position z
- Power overlap integral : intégrale de recouvrement par rapport au champ d'entrée. Ceci peut être très utile si le champ d'entrée est modal, pour mesurer la puissance optique présente *dans le mode guidé* en fonction de z.
- X cut : mesure la puissance optique à une cote X donnée en fonction de z. Cette valeur est normalisée par la puissance en z=0.
- Power in output waveguide : intégrale de recouvrement du champ optique en z maximum avec les champs modaux des guides présents à cet endroit.

Attention : l'ajout de ces mesures augmente le temps de calcul des simulations !

VI - Scripts

Les scripts sont très utiles pour réaliser des simulations complexes, notamment si l'on souhaite faire varier un paramètre. Il est également possible de dessiner une structure et de définir le plan d'entrée uniquement en utilisant un script

Boucle en longueur d'onde :

- Créer un nouveau paramètre : lambda
- Utilisez la commande : Simulation->scanning script. Ceci crée un script contenant une boucle. Ce script est affiché dans un onglet qui s'ajoute aux onglets « layout » et « ref. index ».
- Modifier le script pour faire varier la longueur d'onde de la simulation entre 1 et 2 μm, avec 5 points de mesure. La commande pour modifier un paramètre est :
  ParamMgr.SetParam "*nom_param*", CStr(*variable*)
- **Penser a sauvegarder** après chaque modification du script
- Simulation -> Run script - permet de vérifier que le script ne contient pas d'erreurs
- Simulation -> Calculate 2D isotropic solution
  - Utiliser « lambda » comme longueur d'onde
  - Cocher l'option : simulate using script

Script sur le dessin :

- Effacer tout votre layout et creez un nouveau guide droit (longueur 1mm, largeur w).
- Générer un script de layout (commande : « simulation » -> « generate layout script »)
- Copier ce paragraphe de façon à créer un nouveau guide 5 microns en dessous du premier. Attention : il faut modifier le nom de ce nouveau guide.
- Sauvegarder et lancez la commande « run script ».
- Les scripts permettent donc de créer des guides, ce qui peut être utile combiné à une boucle pour créer automatiquement un layout complexe. Par exemple créer 10 guides espacés de 20 microns et de largeur variant de 1 à 10 microns (il faudra modifier la taille du wafer !)
- *Note* : il est également possible de générer des plans d'entrée à l'intérieur du script.

VII - Mise en pratique sur différentes structures de base

Coupleur :

- Créer 2 guides droits momomodes espacés de 5 microns.
- Mesurez la longueur de couplage du composant
- Comment cette grandeur évolue-t-elle avec la longueur d'onde ? avec l'indice de réfraction des guides ?

Jonction Y :

- Dessinez une jonction Y à base de guides en S (S-bend)

- Les guides doivent être monomodes, la longueur totale de la jonction vaut 1 mm et la séparation des guides de sortie 40 µm
- Tester le bon fonctionnement et évaluer les pertes
- Dessinez une jonction Y inversée, et testez son comportement en recombineur pour différentes injections :
    - Une seule voie excitée
    - 2 voies excitées en phase
    - 2 voies excitées en opposition de phase

Numerical Techniques for Modeling Guided-Wave Photonic Devices

R. Scarmozzino, *Member, IEEE*, A. Gopinath, R. Pregla, *Fellow, IEEE*, and S. Helfert

Invited Paper

***Abstract*—Accurate modeling of photonic devices is essential for the development of new, higher performance optical components required by current and future high-bandwidth communications systems. This paper reviews several key techniques for such modeling, many of which are used in commercial design tools. These include several mode-solving techniques, the beam propagation method, the method of lines, and the finite-difference time-domain technique.**

***Index Terms*—Beam propagation method (BPM), finite difference time domain method (FDTD), method of lines (MoL), modeling, mode solving, photonic devices.**

I. Introduction

RECENT years have seen an enormous increase in bandwidth requirements for telecom and datacom transmission systems due, in large part naturally, to the growth of the Internet. This in turn has put stringent demands on the lightwave transmission systems and the integrated and fiber-optic photonic components that are the foundation of such systems. Conversely, it has been the continual advances in these components [fibers, lasers, detectors, modulators, switches, wavelength-demultiplexing devices (WDM's), etc.], which have enabled systems to meet these ever-increasing demands.

The major contributors to these component advances have of course been the development of novel device concepts and the new or improved technologies enabling their production. Perhaps less apparent to the wider audience, but nonetheless playing an extremely significant role behind the scenes, have been the developments in modeling techniques and the introduction of commercialized computer-aided design (CAD) software for modeling opto-electronic components (and more recently, systems). Design tools and device modeling play several significant roles in the advancement of optical components, including optimization of current designs, shortening of the design cycle for new designs, and evaluation of new device concepts.

Manuscript received September 3, 1999.

R. Scarmozzino is with RSoft, Inc., Ossining, NY 10562 USA (e-mail: rob@rsoftinc.com).

A. Gopinath is with the Electrical and Computer Engineering Department, University of Minnesota, Minneapolis, MN 55455 USA (e-mail: gopinath@ee.umn.edu).

R. Pregla and S. Helfert are with FernUniversität, Allgemeine und Theoretische Elektrotechnik Hagen D-58084 Germany (e-mail: r.pregla@fernuni-hagen.de).

Publisher Item Identifier S 1077-260X(00)01137-0.

Introduced between five to seven years ago, commercialized CAD for component design has become a standard in the industry, with all major and minor component vendors relying on a combination of commercial and in-house tools. These tools would not be possible without the development in modeling techniques for photonics that has occurred over the last two decades. The goal of this paper is to review those techniques that are in widespread use today or are expected to become significant in the near future.

Modeling techniques for optical guided-wave propagation can be divided into two main classes: time-harmonic (e.g., monochromatic CW operation) and general time-dependent (e.g., pulsed operation). Since the optical carrier frequency is so large compared to the bit rate, most devices can be modeled accurately by assuming a monochromatic wave; slower time-dependence can be modeled via Fourier expansion in the time domain using dispersion characteristics obtained from CW modeling. In this context, the most fundamental question to ask is what are the optical modes that can propagate in a given, uniform cross section of a waveguiding structure, and mode-solving techniques for addressing this question are reviewed in Section II. Most photonic devices, however, involve propagation in structures that are nonuniform, and techniques for handling this include the beam propagation method (BPM) and the method of lines (MoL), which are covered in Sections III and IV, respectively. Another important technique that has been employed for nonuniform structures is the well-known coupled mode theory; however, the emphasis in this paper is on predominantly numerical techniques, and thus coupled mode theory is not considered here. Last, the finite-difference time-domain method (FDTD), which is applicable to both CW and pulsed problems, is briefly reviewed in Section V.

II. Mode Solving Techniques

A. Introduction

The dielectric waveguides used in photonic integrated circuits typically need to be single mode, although in many cases multimode or slightly multimode guides are involved in part of the device operation. Thus modal analysis is a critical part of the design process, providing information on the modes that may propagate, their propagation constants and mode shapes, and, via overlap integrals, the relative modal excitations in a multimode guide in response to a given input field. In this section,

several commonly used mode solvers are discussed in some detail. All mode solvers assume that the waveguide section is unaltered in the propagation direction, the z direction, resulting in the assumption that the variation in this direction is as $\exp(i\beta z)$, where β is the propagation constant. The task of mode solvers, for a given waveguide cross-section and a specified value of operating frequency or wavelength, is to determine the values of β and the corresponding modal pattern for each desired mode.

Mode solvers may be classified as scalar wave equation solvers and vector wave equation solvers, with the semi-vectorial being considered as part of the scalar set. The techniques for obtaining the propagation constant for a particular guide section vary, and these naturally fall into several method categories. For the present paper, the method categories are used, but some of the less widely used methods are not described here. For example, the scalar/vector wave equation may be solved analytically in terms of harmonic functions, and then the boundary conditions are imposed to solve for the eigenvalues and vectors of the modes. This approach results in transcendental equation matrices, which require a search algorithm for the embedded eigenvalues. The alternative approach utilizes numerical methods, and here the trial functions satisfy the boundary conditions, and approximately satisfy the governing wave equation. The major methods discussed here are the finite difference and the finite element techniques. Other methods such as the spectral domain technique [1] and the method of lines are not discussed here, although the latter is outlined in Section IV. There are also several mode-solving techniques based on the beam propagation method; these are discussed in Section III.

B. The Finite-Difference Method

From Maxwell's equations, the wave equation in a uniform region of space may be derived to be of the form

$$\nabla^2 \boldsymbol{E} + k_0^2 \varepsilon_r \boldsymbol{E} = 0 \tag{1}$$

where the time harmonic variation of ω is included in k_0^2, which is equal to $\omega^2 \varepsilon_0 \mu_0$, and $\varepsilon_r(x, y)$ is a function describing the relative dielectric constant over the cross-section of the guide. In general, it is assumed that dielectric regions are nonmagnetic, which implies that μ_r is unity over the entire section of the guide. The channel guide, for example in the form of the ridge guide, has different dielectric constants associated with the different layers and the ridge. Thus, ε_r is piecewise constant, and the solution in each region must also satisfy the region's boundary conditions. A similar equation for the $\boldsymbol{H}$ components may also be derived from Maxwell's equations.

Dielectric waveguides can propagate quasi-TE and quasi-TM modes, and therefore the solutions of the wave equation with one component of either the electric or magnetic field provide an approximate scalar solution to the appropriate mode. A solution in which two components of the fields simultaneously satisfy the wave equation, and are coupled through the boundary conditions, is referred to as a vector solution.

In the finite difference method, the domain of analysis is discretized with a rectangular grid of points, which may be of constant or variable spacing. The points may be chosen to lie on the boundaries in which case the boundary conditions are specified by the appropriate central difference formula relating the three grid points, the one on the boundary and the other adjacent ones on each side of the boundary. Alternatively, the points may lie a half step from the boundaries, in which case the boundary condition is set by means of a difference formula involving the two adjacent points across the boundary. A scalar formulation for the quasi-TE mode may be in terms of the E_x or the H_z component, which then implies that the only components present are E_x, H_z, and H_y, and these are related through the Maxwell curl equations. The advantage of the H_z formulation is that no boundary conditions are required to be set on any of the dielectric interfaces, since it is continuous across them. A similar formulation for the TM mode may be in terms of the E_y or E_z component. A vector formulation would have both E_x and E_y present or H_z and E_z present, and the two components of the wave equation have to be solved simultaneously, and these are uncoupled. The dielectric boundary conditions specify continuity of the tangential field components, or the discontinuity of the normal electric field, and consequently the two components become coupled. The second-order wave equation is then discretized by the usual five-point Taylor series formula, and an eigenvalue matrix is assembled. The solution of the resulting eigenvalue problem may be iterative, in which case for convergence the matrix may need to satisfy certain properties depending on the algorithm. Alternatively, sparse matrix routines may be used to obtain the eigenvalues and the corresponding vectors. The domain boundaries usually satisfy Dirichlet or Neumann conditions, although absorbing boundary conditions or perfectly matched boundary conditions may also be introduced. However, in these instances, the media in these special layers are lossy and hence complex, and therefore the matrices become complex, leading to complex eigenvalues that require more sophisticated numerical techniques. A variable mesh with the outside boundaries set to a distance where the fields have become very small is the preferred approach. Alternatively, in the case of methods based on the beam propagation method discussed in Section III, so-called transparent boundary conditions may be employed.

The scalar approach, while providing results of interest, is not accurate for cutoff and propagation constant values, especially for coupled waveguide structures. A paper by Stern [2] modified the quasi-TE scalar formulation in terms of both E_x and E_z and called it the semi-vectorial approach, and found that the results were much more accurate, closer to results obtained from the vector formulations for various channel guides. However, the matrix equation becomes asymmetric, and therefore appropriate matrix routines need to be used to extract the eigenvalues and vectors. A variable spacing mesh approach was used by several authors [3], [4], and the results obtained have been excellent.

Arndt proposed [5] a vector formulation with the transverse $\boldsymbol{H}$ fields, H_x and H_y as the independent variables. The boundary conditions used are the continuity of the transverse components, and the continuity of H_z, and E_z. The H_z component is obtained from the divergence condition for the $\boldsymbol{H}$ fields in each piecewise constant region. Since μ is constant, equal to μ_0, over the whole domain, equating the H_z field from the adjacent regions at the boundary, β cancels out. The expression for E_z does

not contain β, and thus for this formulation the wave equation may be evaluated for β^2. This approach and subsequent papers [6] have shown excellent agreement with other vector solutions.

The finite difference approach solves the discretized second order wave equation, in scalar, semi-vectorial, or vector form. Recasting the equation in variational form would result in a stationary solution to the eigenvalue, and therefore less dependency on the mesh size. Two reports exist in the literature, [7], [8] and here one of these, the latter, is discussed briefly, although it is not strictly variational in formulation. The method is based on an approach suggested by Varga [9], where the wave equation for each component is integrated over a box defined by the half steps in the usual five-point grid. Using the divergence theorem in this integration reduces this to a first-order equation, and the central difference formulas are used to derive the components of the resultant matrix equation. Here again, the coupling of the two components in the vector formulation occurs due to the boundary conditions. In this approach [8], the transverse components of the $\boldsymbol{H}$ vector are used as the independent variables, and the continuity of the H_z and E_z are imposed; these are independent of the propagation constant. Solution of the resultant matrix is accomplished by various routines, and in this paper the Arnoldi method was used, and the results compare very well with published data. If, however, the integration of the wave equation for the particular transverse component H_i is performed with the weighting factor of H_i, then this becomes the variational form, the matrix is symmetrical, and standard matrix routines maybe used to extract the eigenvalues and vectors. Results from [8] show excellent agreement with other calculations.

C. The Finite-Element Method

The finite-element method uses a variational formulation for solution of waveguide problems. For dielectric waveguides, the usual approach is to use all three components of the $\boldsymbol{H}$ or the $\boldsymbol{E}$ vector. The advantage of using the three components of the $\boldsymbol{H}$ field is that no boundary conditions need to be set except at the exterior boundary. From Maxwell's equations

$$\nabla \times \varepsilon_r^{-1}(\nabla \times \boldsymbol{H}) = k_0^2 \boldsymbol{H}. \tag{2}$$

Taking the inner product of this equation with $\boldsymbol{H}^*$ leads to a functional of the form

$$F = \int_S \left[(\nabla \times \boldsymbol{H})^* \cdot \varepsilon_r^{-1}(\nabla \times \boldsymbol{H}) - k_0^2 \boldsymbol{H} \cdot \boldsymbol{H}^*\right] dx\, dy. \tag{3}$$

If the trial function coefficients are a_i, then requiring $\partial F/\partial a_i = 0$ provides the equations for the matrix eigenvalue problem. The trial functions must span the whole domain and satisfy the exterior boundary conditions, and this becomes difficult for arbitrary shapes. Thus, the finite-element method discretizes the domain into a set of contiguous triangles, and the trial functions are defined within each triangle with unknown coefficients. In the nodal element scheme, the trial functions are expressed in the nonorthogonal area coordinates ζ_i, and linear and higher order trial functions in terms of the ζ_i may be used. The integrations of the functional may then be performed for each triangle before the matrix equation is assembled. The problem with the functional in (3) is that spurious eigenvalue modal solutions occur. Furthermore, the formulation requires that β be specified, and the corresponding frequency ω in k_0 is obtained. Since the divergence equation has not been specifically set in this functional, inclusion of this equation in the functional with a summation parameter α mitigates this. While this approach does not eliminate the spurious modes, it pushes them to the higher order modes depending on the choice of α. Some check needs to be made to ensure that the spurious modes are eliminated from the solutions by running the code with different values of α. Using this technique, Rahman and Davies [10] have obtained results on a ridge guide that remain the benchmark against which all other methods are compared. This method has also been used by other groups [11] for modal solutions. Fernandez and Lu [12] modified the functional in terms of transverse $\boldsymbol{H}$ fields, but the problem here is that the matrices are not symmetric, and so extraction of the eigenvalues and vectors is inefficient. Abid *et al.* [13] used the transverse components of the $\boldsymbol{H}$ field Helmholtz equations and set the boundary conditions as in [6] with the null matrix technique to obtain a symmetric eigenvalue matrix equation, but with loss of sparsity.

An improvement on the three component $\boldsymbol{H}$ field method was suggested by Cendes [14], in which the transverse fields are defined by edge elements and the longitudinal field is defined by the usual nodal elements. An edge element between the triangle vertices i, j is defined by

$$\boldsymbol{W}_{\mathrm{ij}} = (\zeta_i \nabla \zeta_j - \zeta_j \nabla \zeta_i) l_{\mathrm{ij}} \tag{4}$$

where:

ζ_i area coordinate defined above;

l_{ij} length of the edge between these vertices.

The result of this definition is that the edge element is a trial function that is along the edge ij. The functional used here is given in (3), and the preferred field set is the components of $\boldsymbol{E}$. With this choice of trial functions, the spurious modes are eliminated. Use of second-order edge elements has given excellent results. Recent work in the finite-element area has focused on the use of edge elements.

III. The Beam Propagation Method

A. Overview

In this section the concept and capabilities of the beam propagation method [15], [16] are reviewed. The BPM is the most widely used propagation technique for modeling integrated and fiber-optic photonic devices, and most commercial software for such modeling is based on it.

There are several reasons for the popularity of BPM; perhaps the most significant being that it is conceptually straightforward, allowing rapid implementation of the basic technique. This conceptual simplicity also benefits the user of a BPM-based modeling tool as well as the implementer, since an understanding of the results and proper usage of the tool can be readily grasped by a nonexpert in numerical methods. In addition to its relative simplicity, the BPM is generally a very efficient method and has the characteristic that its computational complexity can, in most cases, be optimal, that is to say, the computational effort is directly proportional to the number of grid points used in the numerical simulation. Another characteristic of BPM is that

the approach is readily applied to complex geometries without having to develop specialized versions of the method. Furthermore, the approach automatically includes the effects of both guided and radiating fields as well as mode coupling and conversion. Last, the BPM technique is very flexible and extensible, allowing inclusion of most effects of interest (e.g., polarization, nonlinearities) by extensions of the basic method that fit within the same overall framework.

Numerous applications of the BPM to modeling different aspects of photonic devices or circuits have appeared in the literature. Examples from the authors' own experience include various passive waveguiding devices [17], channel-dropping filters [18], electrooptic modulators [19], multimode waveguide devices [20], [21], ring lasers [22], optical delay line circuits [23], [24], novel y-branches [25], optical interconnects [26], polarization splitters [27], multimode interference devices [28]–[32], adiabatic couplers [33], waveguide polarizers [34], and polarization rotators. [35] Most of the above references involve experimental demonstrations of novel device concepts designed in whole or in part via BPM.

In the following subsections, the basic ideas involved in the BPM as well as the main extensions to the technique are explained, and selected theoretical references are given.

B. Scalar, Paraxial BPM

The BPM is essentially a particular approach for approximating the exact wave equation for monochromatic waves, and solving the resulting equations numerically. In this section, the basic approach is illustrated by formulating the problem under the restrictions of a scalar field (i.e., neglecting polarization effects) and paraxiality (i.e., propagation restricted to a narrow range of angles). Subsequent sections will describe how these limitations may be removed.

The scalar field assumption allows the wave equation to be written in the form of the well-known Helmholtz equation for monochromatic waves

$$\frac{\partial^2\phi}{\partial x^2}+\frac{\partial^2\phi}{\partial y^2}+\frac{\partial^2\phi}{\partial z^2}+k(x,\,y,\,z)^2\phi=0. \tag{5}$$

Here the scalar electric field has been written as $E(x,\,y,\,z,\,t)=\phi(x,\,y,\,z)e^{-i\omega t}$, and the notation $k(x,\,y,\,z)=k_0n(x,\,y,\,z)$ has been introduced for the spatially dependent wavenumber, with $k_0=2\pi/\lambda$ being the wavenumber in free space. The geometry of the problem is defined entirely by the refractive index distribution $n(x,\,y,\,z)$.

Aside from the scalar assumption, the above equation is exact. Considering that in typical guided-wave problems the most rapid variation in the field ϕ is the phase variation due to propagation along the guiding axis, and assuming that axis is predominantly along the z direction, it is beneficial to factor this rapid variation out of the problem by introducing a so-called slowly varying field u via the ansatz

$$\phi(x,\,y,\,z)=u(x,\,y,\,z)e^{i\overline{k}z}. \tag{6}$$

Here $\overline{k}$ is a constant number to be chosen to represent the average phase variation of the field ϕ, and is referred to as the reference wavenumber. The reference wavenumber is frequently expressed in terms of a reference refractive index $\overline{n}$, via $\overline{k}=k_0\overline{n}$. Introducing the above expression into the Helmholtz equation yields the following equation for the slowly varying field:

$$\frac{\partial^2u}{\partial z^2}+2i\overline{k}\frac{\partial u}{\partial z}+\frac{\partial^2u}{\partial x^2}+\frac{\partial^2u}{\partial y^2}+(k^2-\overline{k}^2)u=0. \tag{7}$$

At this point, the above equation is completely equivalent to the exact Helmholtz equation, except that it is expressed in terms of u. It is now assumed that the variation of u with z is sufficiently slow so that the first term above can be neglected with respect to the second; this is the familiar slowly varying envelope approximation, and in this context it is also referred to as the paraxial or parabolic approximation. With this assumption and after slight rearrangement, the above equation reduces to

$$\frac{\partial u}{\partial z}=\frac{i}{2\overline{k}}\left(\frac{\partial^2u}{\partial x^2}+\frac{\partial^2u}{\partial y^2}+(k^2-\overline{k}^2)u\right). \tag{8}$$

This is the basic BPM equation in three dimensions (3-D); simplification to two dimensions (2-D) is obtained by omitting any dependence on y. Given an input field $u(x,\,y,\,z=0)$, the above equation determines the evolution of the field in the space $z>0$.

It is important to recognize what has been gained and lost in the above approach. First, the factoring of the rapid phase variation allows the slowly varying field to be represented numerically on a longitudinal grid (i.e., along z) that can be much coarser than the wavelength for many problems, contributing in part to the efficiency of the technique. Second, the elimination of the second derivative term in z reduces the problem from a second-order boundary value problem requiring iteration or eigenvalue analysis, to a first-order initial value problem that can be solved by simple "integration" of the above equation along the propagation direction z. This latter point is also a major factor in determining the efficiency of BPM, implying a time reduction by a factor of at least of the order of N_z (the number of longitudinal grid points) compared to full numerical solution of the Helmholtz equation.

The above benefits have not come without a price. The slowly varying envelope approximation limits consideration to fields that propagate primarily along the z axis (i.e., paraxiality) and also places restrictions on the index contrast (more precisely, the rate of change of index with z, which is a combination of index contrast and propagation angle). In addition, fields that have a complicated superposition of phase variation, such as exist in multimode devices such as MMI's, may not be accurately modeled if the phase variation is critical to device behavior. A second key issue beyond the above restrictions on the variation of u is that the elimination of the second derivative also eliminates the possibility for backward traveling wave solutions; thus devices for which reflection is significant will not be accurately modeled.

Fortunately, the above issues, which should be considered inherent in the BPM approach, can be eliminated or significantly relaxed in many problems through the use of so-called wide-angle and bidirectional extensions to BPM discussed below. Other restrictions in the above formulation, such as neglect of polarization and simplification of materials properties (e.g., isotropic, linear), are not specific to the BPM approach.

Extension of the formulation to address these situations is also considered in subsequent sections. In the following section the numerical solution of the basic BPM equation derived above is considered.

C. Numerical Solution and Boundary Conditions

Equation (8) is a parabolic partial differential equation that can be "integrated" forward in z by a number of standard numerical techniques. Most early BPM's employed a technique known as the split-step Fourier method [15]. Later work demonstrated that for most problems of interest in integrated optics, an implicit finite-difference approach based on the well-known Crank–Nicholson scheme was superior [36]–[38]. This approach and its derivatives have become the standard; thus it is reviewed here. It is frequently denoted FD-BPM in the literature, but will be referred to in the following as simply BPM.

In the finite-difference approach, the field in the transverse (xy) plane is represented only at discrete points on a grid, and at discrete planes along the longitudinal or propagation direction (z). Given the discretized field at one z plane, the goal is to derive numerical equations that determine the field at the next z plane. This elementary propagation step is then repeated to determine the field throughout the structure. For simplicity, the approach is illustrated for a scalar field in 2-D (xz); extension to 3-D is then briefly summarized.

Let u_i^n denote the field at transverse grid point i and longitudinal plane n, and assume that the grid points and planes are equally spaced by Δx and Δz apart, respectively. In the Crank–Nicholson method, (8) is represented at the midplane between the known plane n and the unknown plane $n+1$ as follows:

$$\frac{u_i^{n+1}-u_i^n}{\Delta z}=\frac{i}{2\overline{k}}\left(\frac{\delta^2}{\Delta x^2}+(k(x_i,\, z_{n+1/2})^2-\overline{k}^2)\right)\cdot\frac{u_i^{n+1}+u_i^n}{2}. \tag{9}$$

Here δ^2 represents the standard second order difference operator, $\delta^2 u_i=(u_{i+1}+u_{i-1}-2u_i)$, and $z_{n+1/2}\equiv z_n+\Delta z/2$. The above equation can be rearranged into the form of a standard tridiagonal matrix equation for the unknown field u_i^{n+1} in terms of known quantities, resulting in

$$a_i u_{i-1}^{n+1}+b_i u_i^{n+1}+c_i u_{i+1}^{n+1}=d_i. \tag{10}$$

Expressions for the coefficients in the above are readily derived and can be found in [38]. The tridiagonal nature of (10) allows rapid solution in order $O(N)$ operations, where N is the number of grid points in x.

Since the field can only be represented on a finite computational domain, when the above equation is applied at the boundary points $i=1$ and N it refers to unknown quantities outside the domain. For these points, the above equation must be replaced by appropriate boundary conditions which complete the system of equations. Proper choice of these conditions is critical, since a poor choice can lead to artificial reflection of light incident on the boundary (e.g., radiation) back into the computational domain. For example, simply requiring the field to vanish on the boundary is insufficient since it is equivalent to placing perfectly reflecting walls at the edge of the domain. Several works introduced artificial absorbering material near the edge of the domain; however, adjusting the parameters of the absorber to minimize reflection is cumbersome, and artificial reflections persist in many cases since the interface between the problem space and the absorber will also be partially reflective. A commonly used boundary condition is the so-called transparent boundary condition (TBC) [39], [99]. The basic approach is to assume that near the boundary the field behaves as an outgoing plane wave, with characteristics (amplitude, direction) that are dynamically determined via some heuristic algorithm. The plane wave assumption allows the field at the boundary point to be related to the adjacent interior point, thus completing the set of equations. Details on implementation are given in [39], [99]. The TBC is generally very effective in allowing radiation to freely escape the computational domain; however, there are problems for which it does not perform well. To address this several other boundary conditions have recently been explored [40]–[42].

The above numerical solution can be readily extended to 3-D, however the direct extension of the Crank–Nicholson approach leads to a system of equations that is not tridiagonal, and requires $O(N_x^2 \bullet N_y^2)$ operations to solve directly, which is nonoptimal. Fortunately, there is a standard numerical approach referred to as the alternating direction implicit method [43], which allows the 3-D problem to be solved with optimal $O(N_x \bullet N_y)$ efficiency.

In this and the previous section the concept and implementation details of the basic BPM method have been reviewed. In the following sections various methods for extending the BPM are summarized, and details of numerical implementation can be found in the corresponding references.

D. Including Polarization—Vector BPM

Polarization effects can be included in the BPM by recognizing that the electric field $\boldsymbol{E}$ is a vector, and starting the derivation from the vector wave equation rather than the scalar Helmholtz equation [44], [45]. In one approach, the equations are formulated in terms of the transverse components of the field (E_x and E_y), and result in the following set of coupled equations for the corresponding slowly varying fields (u_x and u_y) [45]:

$$\frac{\partial u_x}{\partial z}=A_{\rm xx}u_x+A_{\rm xy}u_y \tag{11}$$

$$\frac{\partial u_y}{\partial z}=A_{\rm yx}u_x+A_{\rm yy}u_y. \tag{12}$$

The $A_{\rm ij}$ are complex differential operators given by

$$\begin{aligned}
A_{\rm xx}u_x&=\frac{i}{2\overline{k}}\left\{\frac{\partial}{\partial x}\left[\frac{1}{n^2}\frac{\partial}{\partial x}(n^2u_x)\right]+\frac{\partial^2}{\partial y^2}u_x+(k^2-\overline{k}^2)u_x\right\}\\
A_{\rm yy}u_y&=\frac{i}{2\overline{k}}\left\{\frac{\partial^2}{\partial x^2}u_y+\frac{\partial}{\partial y}\left[\frac{1}{n^2}\frac{\partial}{\partial y}(n^2u_y)\right]+(k^2-\overline{k}^2)u_y\right\}\\
A_{\rm yx}u_x&=\frac{i}{2\overline{k}}\left\{\frac{\partial}{\partial y}\left[\frac{1}{n^2}\frac{\partial}{\partial x}(n^2u_x)\right]-\frac{\partial^2}{\partial y\partial x}u_x\right\}\\
A_{\rm xy}u_y&=\frac{i}{2\overline{k}}\left\{\frac{\partial}{\partial x}\left[\frac{1}{n^2}\frac{\partial}{\partial y}(n^2u_y)\right]-\frac{\partial^2}{\partial x\partial y}u_y\right\}.
\end{aligned} \tag{13}$$

The operators A_{xx} and A_{yy} account for polarization dependence due to different boundary conditions at interfaces and describe such effects as different propagation constants, field shapes, bend loss, etc., for TE and TM fields. The off-diagonal terms involving A_{xy} and A_{yx} account for polarization coupling and hybrid modes due to geometric effects, such as the influence of corners or sloping walls in the cross-sectional structure (effects due to material anisotropy are considered below).

The above equations are generally referred to as describing a full-vectorial BPM. The simplification $A_{xy} = A_{yx} = 0$ gives the important semi-vectorial approximation. In this case the transverse field components are decoupled, simplifying the problem considerably while retaining what are usually the most significant polarization effects. Unless a structure is specifically designed to induce coupling, the effect of the off-diagonal terms is extremely weak and the semi-vectorial approximation is an excellent one.

E. Removing Paraxiality—Wide-Angle BPM

The paraxiality restriction on the BPM, as well as the related restrictions on index-contrast and multimode propagation noted earlier, can be relaxed through the use of extensions that have been referred to as wide-angle BPM [46]–[48], [100]. The essential idea behind the various approaches is to reduce the paraxial limitations by incorporating the effect of the $\partial^2 u/\partial z^2$ term that was neglected in the derivation of the basic BPM. The different approaches vary in the method and degree of approximation by which they accomplish this. The most popular formulation is referred to as the multistep Padé-based wide-angle technique [47], [100], and is summarized below.

A simple approach for deriving a wide-angle BPM equation is to consider the Helmholtz wave equation written in terms of the slowly varying field (7), but before the making the slowly varying envelope approximation by neglecting the $\partial^2 u/\partial z^2$term. If D denotes $\partial/\partial z$ in this equation, then $\partial^2/\partial z^2$ is represented by D^2. Putting aside the fact that D is a differential operator, the equation can now be viewed as a quadratic equation to be solved for D, yielding the following formal solution for a first-order equation in z:

$$\frac{\partial u}{\partial z} = i\bar{k}\left(\sqrt{1+P}-1\right)u \tag{14}$$

$$P \equiv \frac{1}{\bar{k}^2}\left(\frac{\partial^2}{\partial x^2}+\frac{\partial^2}{\partial y^2}+(k^2-\bar{k}^2)\right). \tag{15}$$

This equation is referred to as a one-way wave equation, since the first-order derivative admits only forward traveling waves (or backward waves if the signs are chosen appropriately, but not both simultaneously). Although restricted to forward propagation, the above equation is still exact in that no paraxiality approximation has been made. The difficulty is that before this equation can be integrated the radical involving the differential operator P must be evaluated. One approach would be to use a Taylor expansion. To first order this leads to the standard paraxial BPM, and to higher order it becomes more accurate and represents one approach to achieving a wide-angle scheme. However expansion via Padé approximants is more accurate than the Taylor expansion for the same order of terms [47], [100]. This approach leads to the following wide-angle equation [47], [100]:

$$\frac{\partial u}{\partial z} = i\bar{k}\frac{N_m(P)}{D_n(P)}u. \tag{16}$$

Here N_m and D_n are polynomials in the operator P and (m, n) is the order of the approximation. Table I shows several common approximants. When (16) is employed, larger angles, higher index contrast, and more complex mode interference can be analyzed in both guided wave and free space problems as the Padé, order (m, n) is increased [47], [49], [100]. Guidelines for using the technique and a discussion of the complex interrelationships between waveguide angle, index contrast, Padé order, reference wavenumber, and grid parameters are discussed in [49].

TABLE I

Padé Order (m,n)	N_m	D_n
(1,0)	$P/2$	1
(1,1)	$P/2$	$1+P/4$
(2,2)	$P/2+P^2/4$	$1+3P/4+P^2/16$

F. Handling Reflections—Bidirectional BPM

While wide-angle BPM allows propagation in a wider cone of angles about the z axis, this cone can only asymptotically approach ±90° from the z axis and can never be extended to handle simultaneous propagation along the negative z axis (i.e., 180°). For this, one must treat the backward traveling waves as a separate, though coupled, part of the problem. Various bidirectional BPM techniques have been considered to address this issue [50]–[52] with most focusing on the coupling that occurs through reflection of a wave incident on an interface along z. Here a recent technique that considers multiple interfaces and reflections in a self-consistent and efficient way is reviewed [53].

In this method, the guided wave propagation problem is divided into regions that are uniform along z and the interfaces between these regions (problems involving curved sections can be described in this way via a stair-step approximation). At any point along the structure it is considered that both forward and backward waves can exist, which are denoted by $u^+(x, y, z)$ and $u^-(x, y, z)$, respectively. In the uniform regions the forward and backward waves are decoupled, while the interfaces between these regions couple the forward and backward waves due to reflection.

The essential idea in [53] is to employ a transfer matrix approach in which the individual matrices are differential operators. The physical problem generally has the incident (forward) field given at the input of the structure, and the goal is to determine the reflected (backward) field at the beginning and the transmitted (forward) field at the output. The transfer matrix problem, however, is formulated by assuming that both the forward and backward fields are known at the input of the structure, and an overall transfer matrix M then describes the system as follows:

$$\begin{pmatrix} u^+_{\text{out}} \\ u^-_{\text{out}} \end{pmatrix} = M \begin{pmatrix} u^+_{\text{in}} \\ u^-_{\text{in}} \end{pmatrix}. \tag{17}$$

Given incident field (u_{in}^{+}), the above is solved iteratively for reflected field (u_{in}^{-}) such that the backward field at the output is zero ($u_{\text{out}}^{-} = 0$). The transfer matrix M describing the entire structure is composed of successive applications of propagation and interface matrices. The propagation matrices describe the uniform regions and propagate u^{+} and u^{-} independently using normal BPM (either paraxial or wide-angle depending on the situation). The interface matrices relate u^{+} and u^{-} across an interface and are given by generalized Fresnel formulas involving differential operators employing the Padé approximants used in wide-angle BPM [53].

G. Additional BPM Techniques

There are several additional BPM techniques worth noting. First, while the above discussion has focused on linear, isotropic materials, it is possible to include nonlinear or anisotropic material effects in the BPM as well. Most anisotropic materials are readily dealt with in the context of the full-vectorial BPM described above by extending the definition of the operators A_{ij} to account for the fact that material index is described by a dielectric tensor [54].

Nonlinear materials can be accommodated by allowing the refractive index appearing in the equations to be a function of the optical field intensity. Only a small adjustment is required in the solution of the resulting finite-difference equations to account for the fact that the index is a function of the unknown field at the next z step. A simple iteration procedure allows a self-consistent solution to the nonlinear difference equations to be obtained, usually in one or two iterations.

Other areas of recent interest in BPM modeling are the use of higher order numerical schemes [55], [56], and the related issue of accurately dealing with dielectric interfaces [57], [58].

H. Mode Solving Via BPM

Before leaving the subject of BPM, it is worth noting that several useful mode-solving techniques have been developed that are based on BPM; thus a code written to do BPM propagation can be turned into a mode-solver in a relatively straightforward manner. The earliest of these is referred to here as the correlation method and was used to calculate modes and dispersion characteristics of multimode fibers [59]. More recently, a technique referred to as the imaginary distance BPM has been developed, which is generally significantly faster [60], [61]. It should be noted that the imaginary distance BPM technique is formally equivalent to many other iterative mode solving techniques [62], [63]; the description in terms of BPM is simply a convenience that allows one to leverage existing code and concepts. The results in [63], which can be duplicated via imaginary distance BPM, have shown excellent agreement with other published data.

In both BPM-based mode-solving techniques a given incident field is launched into a geometry that is z-invariant, and some form of BPM propagation is performed. Since the structure is uniform along z, the propagation can be equivalently described in terms of the modes and propagation constants of the structure. Considering 2-D propagation of a scalar field for simplicity, the incident field $\phi_{\text{in}}(x)$ can be expanded in the modes of the structure as

$$\phi_{\text{in}}(x) = \sum_{m} c_m \phi_m(x). \tag{18}$$

The summation should of course consist of a true summation over guided modes and integration over radiation modes, but for brevity the latter is not explicitly shown. Propagation through the structure can then be expressed as

$$\phi(x, z) = \sum_{m} c_m \phi_m(x) e^{i\beta_m z}. \tag{19}$$

In each BPM-based mode-solving technique, the propagating field obtained via BPM is conceptually equated with the above expression to determine how to extract mode information from the BPM results.

As the name implies, in the imaginary distance BPM the longitudinal coordinate z is replaced by $z' = iz$, so that propagation along this imaginary axis should follow

$$\phi(x, z') = \sum_{m} c_m \phi_m(x) e^{\beta_m z'}. \tag{20}$$

The propagation implied by the exponential term in (19) has become exponential growth in (20), with the growth rate of each mode being equal to its real propagation constant. The essential idea of the method is to launch an arbitrary field, say a Gaussian, and propagate the field through the structure along the imaginary axis. Since the fundamental mode ($m = 0$) has by definition the highest propagation constant, its contribution to the field will have the highest growth rate and will dominate all other modes after a certain distance, leaving only the field pattern $\phi_0(x)$. The propagation constant can then be obtained by the following variational-type expression:

$$\beta^2 = \frac{\int \phi^* \left(\dfrac{\partial^2 \phi}{\partial x^2} + k^2 \phi \right) dx}{\int \phi^* \phi \, dx}. \tag{21}$$

Higher order modes can be obtained by using an orthogonalization procedure to subtract contributions from lower order modes while performing the propagation [64]. Issues such as optimal choice of launch field, reference wavenumber, and step size are discussed in [61] and [63].

It is important to note that the imaginary distance BPM is not the same as the common technique of performing a standard propagation and waiting for the solution to reach steady state. The latter will only obtain the fundamental mode if the structure is single mode, and generally takes longer to converge. The imaginary distance BPM is closely related to the shifted inverse power method for finding eigenvalues and eigenvectors of a matrix.

In the correlation method, an arbitrary field is launched into the structure and propagated via normal BPM. During the propagation the following correlation function between the input field and the propagating field is computed:

$$P(z) = \int \phi_{\text{in}}^{*}(x) \phi(x, z) \, dx. \tag{22}$$

Using (18) and (19), the correlation function can also be expressed as

$$P(z) = \sum_{m} |c_m|^2 e^{i\beta_m z}. \tag{23}$$

From this expression one can see that a Fourier transform of the computed correlation function should have a spectrum with peaks at the modal propagation constants. The corresponding modal fields can be obtained with a second propagation by beating the propagating field against the known propagation constants via

$$\phi_m(x) = \frac{1}{L}\int_0^L \phi(x, z)e^{-i\beta_m z}. \tag{24}$$

Further details on the technique are found in [59]. While the correlation method is generally slower than the imaginary distance BPM, it has the advantage that it is sometimes applicable to problems that are difficult or impossible for imaginary distance BPM, such as leaky or radiating modes.

IV. The Method of Lines

A. Background

The method of lines is a semi-analytical algorithm for solving partial differential equations such as occur, for example, in electromagnetic field problems in microwaves or optics. It is connected with the mode matching technique (MMT) and with the finite-difference method (FDM). As in the MMT, eigensolutions are used to describe the field. These eigensolutions are not obtained by series expansions but by discretization. In contrast to the FDM, the discretization is not done completely but only as far as necessary in order to transform the partial differential equations to ordinary ones that will be solved analytically. The MoL has monotonic convergence behavior. Difficulties such as relative convergence and spurious mode solutions do not exist.

The MoL has the advantages of the FDM in the discretization directions. Discontinuities in the analytical direction can be taken into account with high accuracy. In optical components radiation can take place, and by introducing absorbing boundary conditions (ABC), it is very easy to model this radiation in the MoL. In contrast, as yet radiation cannot be modeled by MMT in a finite domain since the Dirichlet or Neumann boundary conditions typically used in MMT can never model radiation correctly.

The basics of the MoL are described in [65]. The analysis of longitudinally varying structures is described in [66]–[68, ch. 2.2]. This latter algorithm has also been named MoL-BPM, because it contains some principles that were used in the beam propagation method developed by Feit and Fleck [15].

For obtaining a numerically stable algorithm, the impedance/admittance transformation formulas have been developed [65], [69], [70]. Combining this impedance transformation formulas with Floquet's theorem leads to an algorithm that allows the analysis of periodic structures with a very high number of periods without any numerical problems and with a very low numerical effort [71]. For example, the analysis of a Bragg-grating consisting of some 10 000 periods is described in [71]. This method could also be used for the study of linear and nonlinear fiber-gratings [72].

The impedance transformation principle has also later been applied in the film-mode-matching method [73]. Its combination with the Floquet algorithm in other bidirectional eigenmode algorithms is described in [74].

The MoL with Cartesian coordinates has been used to model eigenmodes of optical waveguides [75], [69], nonlinear material [76], anisotropic-material [70], [77], polarization converters [78], y-branches [79], and sharp bends [80]. By concatenating sharp bends, curved waveguides can also be modeled [81], [82]. For analysis of non-Cartesian problems, formulas in other coordinate systems have been developed. For example, using cylindrical coordinates devices such as curved waveguides [83]–[87], tapers [88], fibers [72], and vertical cavity surface emitting lasers (VCSEL's) have been examined [89].

For analyzing VCSEL's, in addition to the electromagnetic problem, the distributions of the temperature and the current also have to be computed. The partial differential equations for these problems could be solved with the MoL as well [89].

To reduce the numerical effort in case of thin dielectric or metal layers, formulas for the finite differences in these special cases have been developed [90], [91]. With these expressions, no discretization point has to be placed within the thin layer, allowing a coarse grid. The formulas can also be applied in FD-BPM algorithms.

B. Theory

In this section, the application of the MoL to the analysis of propagation problems for 2-D devices is described. The solution for 3-D devices or the solution of eigenvalue problems can be found in the literature given above. As in the case of the BPM described above, monochromatic waves with harmonic time-dependence are assumed; however, for consistency with the literature, the implicit time-dependence has been assumed to have the opposite sign, namely, $e^{i\omega t}$.

The principles will be demonstrated for so-called slab or film waveguides (see Fig. 1). The structure under study may be inhomogeneous in the propagation (z) and transverse (x) directions. The complete field distribution is obtained by a superposition of the TM_z and TE_z modes. The fields are y independent and can be obtained from the y-components H_y (TM) andE_y (TE), respectively. These field components have to fulfill the following Helmholtz wave equations:

TM-modes:

$$\frac{\partial^2 \tilde{H}_y}{\partial \overline{z}^2} + \varepsilon_{rx}\frac{\partial}{\partial \overline{x}}\left(\varepsilon_{rz}^{-1}\frac{\partial}{\partial \overline{x}}\tilde{H}_y\right) + \varepsilon_{rx}\tilde{H}_y = 0$$

TE-modes:

$$\frac{\partial^2 E_y}{\partial \overline{z}^2} + \frac{\partial^2 E_y}{\partial \overline{x}^2} + \varepsilon_{ry}E_y = 0. \tag{25}$$

Here, $\varepsilon_{ri} = n_i(x, z)^2$ are the relative dielectric constants ($\overleftrightarrow{\varepsilon}_r = \mathrm{diag}(\varepsilon_{rx}, \varepsilon_{ry}, \varepsilon_{rz})$), and the following normalizations have been introduced: $\overline{x} = k_0 x$, $\overline{z} = k_0 z$, and $\tilde{H}_y = \eta_0 H_y$, where k_0 and η_0 are the free space wavenumber and wave impedance, respectively. The remaining field components are calculated in the usual manner from curl Maxwell equations.

To solve the above partial differential equations (25) by the method of lines, they are first converted to ordinary differential equations by means of a discretization. Wave propagation is assumed to be in the z direction; therefore discretization is performed in the$x$ direction. The discretization lines are sketched in Fig. 1. A system of two discretization lines is used to fulfill

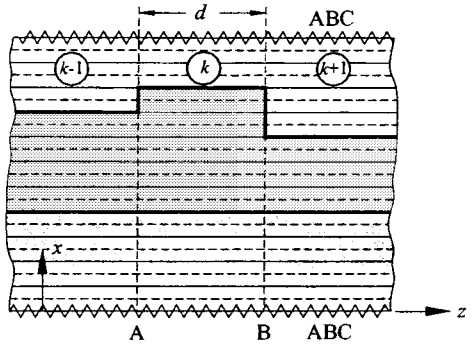

Fig. 1. Concatenation of film waveguide sections with discretization lines used in the MoL. h – – – $H_y, E_x, H_z, \varepsilon_h$(TM). $eE_y, H_x, E_z, \varepsilon_e$(TE).

the boundary conditions for the TM-TE case [65], [67]. The discretization yields

$$\begin{gathered}\tilde{H}_y \rightarrow \tilde{\boldsymbol{H}}_{\boldsymbol{y}} \\ \varepsilon_{rx}, \varepsilon_{rz} \rightarrow \boldsymbol{\varepsilon}_x, \boldsymbol{\varepsilon}_z \\ \frac{\partial \tilde{H}_y}{\partial \overline{x}} \rightarrow \overline{h}^{-1} \boldsymbol{D}_h \tilde{\boldsymbol{H}}_{\boldsymbol{y}} = \overline{\boldsymbol{D}}_h \tilde{\boldsymbol{H}}_{\boldsymbol{y}} \\ \tilde{E}_y \rightarrow \tilde{\boldsymbol{E}}_{\boldsymbol{y}} \\ \varepsilon_{ry} \rightarrow \boldsymbol{\varepsilon}_y \\ \frac{\partial \tilde{E}_y}{\partial \overline{x}} \rightarrow \overline{h}^{-1} \boldsymbol{D}_e \tilde{\boldsymbol{E}}_{\boldsymbol{y}} = \overline{\boldsymbol{D}}_e \tilde{\boldsymbol{E}}_{\boldsymbol{y}}.\end{gathered} \tag{26}$$

The values of the field components on the discretization lines are collected in column vectors, and the values of the discretized permittivities in diagonal matrices. The differential operators are approximated by difference operator matrices $\boldsymbol{D}$. The subscripts correspond to the component (e.g., $H_y \rightarrow$ h-line system: subscript h) from which all the field components are obtained. For the TM$_z$ case, the permittivity $\varepsilon_r(x)$ must be discretized on both line systems. The difference matrices have the form shown in [67] and can incorporate different boundary conditions based on the values in the first and last lines.

The discretized derivatives with respect to z and the permittivity are now combined in operator matrices

$$\boldsymbol{Q}_e = \boldsymbol{\varepsilon}_x \overline{\boldsymbol{D}}_h^t \boldsymbol{\varepsilon}_z^{-1} \overline{\boldsymbol{D}}_h^{(a)} - \boldsymbol{\varepsilon}_x \quad \boldsymbol{Q}_h = \overline{\boldsymbol{D}}_e^t \overline{\boldsymbol{D}}_e^{(a)} - \boldsymbol{\varepsilon}_y$$

resulting in the discretized wave equation

$$\frac{d}{d\overline{z}^2} \Psi - \boldsymbol{Q} \Psi = 0. \tag{27}$$

Ψ and $\boldsymbol{Q}$ stand for the particular transverse field component (H_y or E_y) and operator matrix, respectively. $\overline{\boldsymbol{D}}^t$ is the transpose of matrix $\overline{\boldsymbol{D}}$. $\boldsymbol{D}^{(a)}$ refers to the difference operator with absorbing boundary conditions (see [67]).

Since (27) is a coupled differential equation system, a transformation to principle axes is required

$$\boldsymbol{T}^{-1} \boldsymbol{Q} \boldsymbol{T} = \Gamma^{-1} \quad \Psi = \boldsymbol{T} \overline{\Psi}$$

resulting in the following decoupled differential equation system:

$$\frac{d}{d\overline{z}^2} \overline{\Psi} - \Gamma^2 \overline{\Psi} = 0$$

with the analytical solution

$$\overline{\Psi}(z) = e^{-\Gamma \overline{z}} \overline{\Psi}_f(0) + e^{\Gamma \overline{z}} \overline{\Psi}_b(0). \tag{28}$$

The subscripts f and b indicate that the solution consists of a forward and a backward propagating part.

Now, introducing the fields in the transformed domain according to

$$\begin{aligned} \overline{\boldsymbol{H}}_y &= \boldsymbol{T}_e^{-1} \boldsymbol{H}_y \quad & \overline{\boldsymbol{E}}_y &= \boldsymbol{T}_h^{-1} \boldsymbol{E}_y \\ \overline{\boldsymbol{E}}_x &= \boldsymbol{T}_e^{-1} \boldsymbol{\varepsilon}_x \boldsymbol{E}_x \quad & \overline{\boldsymbol{H}}_x &= \boldsymbol{T}_h^{-1} \boldsymbol{H}_x \end{aligned}$$

a relation between the fields at cross sections $\boldsymbol{A}$ and $\boldsymbol{G}$ of a homogeneous region (see Fig. 1) can easily be derived

$$\begin{bmatrix} \overline{\boldsymbol{E}}_A \\ \overline{\boldsymbol{E}}_B \end{bmatrix} = \begin{bmatrix} \overline{z}_1 & \overline{z}_2 \\ \overline{z}_2 & \overline{z}_1 \end{bmatrix} \begin{bmatrix} \upsilon \overline{\boldsymbol{H}}_A \\ -\upsilon \overline{\boldsymbol{H}}_B \end{bmatrix} \tag{29}$$

with $\upsilon = 1(-1)$ in the TM– (TE–) case and

$$\begin{aligned} \overline{z}_{1e,h} &= \overline{Z}_{0e,h} (\tanh(\Gamma_{e,h} \overline{d}))^{-1} \\ \overline{z}_{2e,h} &= \overline{Z}_{0e,h} (\sinh(\Gamma_{e,h} \overline{d}))^{-1}. \end{aligned}$$

$\overline{d}$ is the normalized length of the waveguide between planes $\boldsymbol{A}$ and $\boldsymbol{B}$ (Fig. 1). The characteristic impedance matrices $\overline{Z}_{0e,h}$ are given by

$$\overline{\boldsymbol{Z}}_{0\mathrm{h}} = -j\Gamma_{\mathrm{h}} \quad \overline{\boldsymbol{Z}}_{0\mathrm{e}} = j\Gamma_{\mathrm{e}}^{-1}$$

and the admittance is defined by

$$\overline{\boldsymbol{Y}}_{0\mathrm{h,e}} = \overline{\boldsymbol{Z}}_{0\mathrm{h,e}}^{-1}.$$

If impedance matrices in cross sections $\boldsymbol{A}, \boldsymbol{B}$ inside section k are defined according to

$$\overline{\boldsymbol{E}}_{\mathrm{A,B}} = \overline{\boldsymbol{Z}}_{\mathrm{A,B}} \overline{\boldsymbol{H}}_{A,B} \tag{30}$$

the following impedance transfer formula can be derived from (29):

$$\overline{\boldsymbol{Z}}_{\mathrm{A}} = \overline{z}_1 - \overline{z}_2 (\overline{z}_1 + \overline{\boldsymbol{Z}}_{\mathrm{B}})^{-1} \overline{z}_2. \tag{31}$$

Thus, if an impedance $\overline{Z}_B$ is defined in the cross section $\boldsymbol{B}$, (31) describes how this impedance is transformed to cross section $\boldsymbol{A}$ of the section labeled k (see Fig. 1). If the length of the device becomes infinity ($d \rightarrow \infty$), $\overline{z}_2$ approaches zero and $\overline{z}_1$ approaches the characteristic impedance matrix $\overline{Z}_0$. At the concatenation of different sections (e.g., sections k and $k+1$ in plane $\boldsymbol{B}$) the fields and therefore the impedances must be matched. This yields

$$\overline{\boldsymbol{Z}}_B^{\boldsymbol{k}} = \boldsymbol{T}_{\boldsymbol{k}}^{-1} \boldsymbol{\nu}_{\boldsymbol{k}} \boldsymbol{T}_{\boldsymbol{k+1}} \overline{\boldsymbol{Z}}_B^{\boldsymbol{k+1}} \boldsymbol{T}_{\boldsymbol{k+1}}^{-1} \boldsymbol{T}_{\boldsymbol{k}} \tag{32}$$

with $\nu_{e,k} = I$ (identity matrix) for the TE-case and $\nu_{h,k} = \varepsilon_{x,k} \varepsilon_{x,k+1}^{-1}$ for the TM-polarization. Now a complete analysis of a complex structure is possible. Starting at the end of the structure the load impedance is transformed through the various sections using (31) and (32). In the case of an infinite waveguide section at the end, the load impedance matrix is the characteristic impedance matrix (30) of this infinite waveguide section. Now injecting a field at the input of the structure, the reflected, the transmitted, and the total field can be computed from the input impedance and this incident wave. To avoid numerical problems when determining the field distribution inside the device, the exponentially increasing term in (28) is not used. Instead, the impedances that were calculated in the previous step of the analysis are combined with the forward propagating part of the field. For a detailed description of this procedure, we refer to the literature [92].

If multiple reflections can be neglected only the computation of the forward propagating fields is required, resulting in

$$\Psi(z) = \boldsymbol{T} e^{-\Gamma \overline{z}} \overline{\Psi}_f(0) = \boldsymbol{T} e^{-\Gamma \overline{z}} \overline{\Psi}(0). \tag{33}$$

At concatenations of different sections, the matching process results in the following formula for the transmitted field:

$$\overline{\Psi}_{k+1} = 2\left(\boldsymbol{T}_k^{-1}\boldsymbol{T}_{k+1} + \overline{\boldsymbol{W}}_{0,k}^{-1}\boldsymbol{T}_k^{-1}\nu_k\boldsymbol{T}_{k+1}\overline{\boldsymbol{W}}_{0,k+1}\right)^{-1}\overline{\Psi}_k$$

with

$$\overline{\boldsymbol{W}}_{\mathbf{o}} = \begin{cases} \overline{\boldsymbol{Z}}_{\mathbf{o}}(\mathrm{TM}) \\ \overline{\boldsymbol{Y}}_{\mathbf{o}}(\mathrm{TE}) \end{cases}.$$

However, multiple reflections are neglected in this simpler algorithm. If no reflections at all must be considered, the procedure can be simplified further. For the propagation of the fields in homogeneous sections again (33) is used. In contrast, at interfaces between different sections the formula

$$\overline{\Psi}_{k+1} = \boldsymbol{T}_{k+1}^{-1}\boldsymbol{T}_k\overline{\Psi}_k$$

is applied. The last formula is similar to those usually used in FD-BPM algorithms. It was also implemented in the earliest MoL-BPM algorithm [66]. Simplifying the formulas results in less matrix-inversions, and thus in a reduction of the numerical effort. However, it should be mentioned that this reduction of the numerical effort also leads to a loss of accuracy for problems in which reflection is important.

In summary, the MoL is very efficient and accurate even for very long and complex devices. This is because the MoL follows the natural wave propagation. The impedance/admittance transformation is a direct consequence of this fact.

V. The Finite-Difference Time-Domain Method

The FDTD technique represents a widely used propagation solution technique in integrated optics, especially in photonic bandgap device computations where the beam propagation solutions are inadequate, or cannot cope with the geometry. The major limitation is that the three-dimensional version requires large storage and extremely long computation times. The basic technique has been outlined in several papers and books devoted to the technique, for example, [93] and [94]. The solution of the wave propagation is by direct integration in the time domain of the Maxwell curl equations in discretized form. For example, the z component of the curl $\boldsymbol{H}$ equation is given by

$$\left[\frac{\partial H_y}{\partial x} - \frac{\partial H_x}{\partial y}\right] = \frac{\partial D_z}{\partial t}. \tag{34}$$

Discretizing via central differences in time and space gives (35), shown at the bottom of the page. The grid is staggered in time and space (the so-called Yee mesh following [93]), and the equations for the other field components follow this form. With a given excitation at the input either in CW or pulsed form, the excitation may be propagated through the structure by time stepping through the entire grid repeatedly. This first-order difference formulation is second-order accurate. In the interest of time and computational speed, most of the computations in the integrated optics area are in two dimensions. A large number of papers of applications in integrated optics are available in the literature, especially in the integrated photonic research meeting abstracts. Higher order formulations are also available but the overhead that is carried slows down the marching algorithm, while improving accuracy for a specific grid size. The integrated form of the curl equations leads to a finite volume formulation. Again, a marching algorithm is developed on a split grid, as above.

A recent two-dimensional alternative to the above first-order formulation, as applied to optical guides, is the higher order compact algorithm based on the split operator technique of Strang [95] and Shang [96]. In this approach, two fields, for example, E_z and B_x, are combined to define a Riemann time invariant variable, and the propagation of this variable uses the piecewise parabolic approximation suggested by Woodward and Colella [97]. Further details of this approach may be obtained from [98]. Since the algorithm is two-dimensional the run times are smaller, and because of the parabolic approximation, higher order accuracy is obtained without the overhead of the higher order formulation.

VI. Conclusion

Modeling techniques for guided-wave photonic devices have developed considerably over the last two decades. These advances, coupled with a rapid increase in available computing power, have allowed practical commercial modeling tools for opto-electronics to be developed and to become a standard within the photonics industry. Further advancement and adoption of such tools will be an integral part of the growth of the photonics industry as it matures toward the size and significance of the current electronics industry.

Acknowledgment

The authors would like to thank E. Heller and H. Rao for their assistance in reviewing the manuscript.

$$\varepsilon\left[\frac{E_z^{t+\Delta t}(x,y,z) - E_z^{t}(x,y,z)}{\Delta t}\right] = \left[\frac{H_y^{t+\Delta t/2}(x+\Delta x/2,y,z) - H_y^{t+\Delta t/2}(x-\Delta x/2,y,z)}{\Delta x}\right] - \left[\frac{H_x^{t+\Delta t/2}(x,y+\Delta y/2,z) - H_x^{t+\Delta t/2}(x,y-\Delta y/2,z)}{\Delta y}\right] \tag{35}$$

REFERENCES

[1] P. McIlroy, M. S. Stern, and P. C. Kendal, "Spectral index method for polarized modes in semiconductor rib waveguides," *J. Lightwave Technol.*, vol. 8, pp. 113–117, 1990.

[2] M. S. Stern, "Semivectorial polarized finite difference method for optical waveguides with arbitrary index profiles," *Proc. Inst. Elect. Eng.*, vol. 135, pp. 56–63, 1993.

[3] S. Seki, T. Yamanaka, and K. Yokoyama, "Two-dimensional analysis of optical waveguides with a nonuniform finite difference method," *Proc. Inst. Elect. Eng.*, vol. 138, pp. 123–127, 1991.

[4] K. L. Johnson, "Nonuniform semivectorial finite difference analysis of dielectric optical waveguide structures," M.S. thesis, University of Minnesota, Department of Electrical Engineering, 1993.

[5] K. Bierwirth, N. Schulz, and F. Arndt, "Finite difference analysis of rectangular dielectric waveguide structures," *IEEE Trans. Microwave Theory Tech.*, vol. MTT-34, pp. 1104–1113, 1986.

[6] N. Schulz, K. Bierwirth, and F. Arndt, "Finite difference method without spurious solutions for the hybrid mode analysis of diffused channel waveguides," *IEEE Trans. Microwave Theory Tech.*, vol. 38, pp. 722–729, 1990.

[7] R. K. Lagu and R. V. Ramaswamy, "A variational finite-difference method for analyzing channel waveguides with arbitrary index profiles," *IEEE J. Quantum Electron.*, vol. QE-22, pp. 968–976, 1986.

[8] H. Dong, A. Chronopoulos, J. Zou, and A. Gopinath, "Vectorial integrated finite difference analysis of dielectric waveguides," *J. Lightwave Technol.*, vol. 11, pp. 1559–1564, 1993.

[9] R. Varga, *Matrix Iterative Analysis*. Englewood Cliffs, NJ: Prentice-Hall, 1962.

[10] B. A. M. Rahman and J. B. Davies, "Finite element analysis of optical and microwave problems," *IEEE Trans. Microwave Theory Tech.*, vol. MTT-32, pp. 20–28, 1983.

[11] M. Koshiba, K. Hayata, and M. Suzuki, "Improved finite element formulation in terms of the magnetic fields vector for dielectric waveguides," *IEEE Trans. Microwave Theory Tech.*, vol. MTT-33, pp. 227–233, 1985.

[12] F. A. Fernandez and Y. Lu, "Variational finite element analysis of dielectric waveguides with no spurious solutions," *Electron. Lett.*, vol. 26, pp. 2125–2126, 1990.

[13] Z.-E. Abid, K. L. Johnson, and A. Gopinath, "Analysis of dielectric guides by vector transverse magnetic fields finite elements," *J. Lightwave Technol.*, vol. 11, pp. 1543–1549, 1993.

[14] J. F. Lee, D. K. Sun, and Z. J. Cendes, "Full wave analysis of dielectric waveguides using tangential finite elements," *IEEE Trans. Microwave Theory Tech.*, vol. MTT-39, pp. 1262–1271, 1991.

[15] M. D. Feit and J. A. Fleck, "Light propagation in graded-index optical fibers," *Appl. Opt.*, vol. 17, pp. 3990–3998, 1978.

[16] D. Yevick, "A guide to electric field propagation techniques for guided-wave optics," *Opt. Quantum Electron.*, vol. 26, pp. S185–S197, 1994.

[17] L. Eldada, M. N. Ruberto, R. Scarmozzino, M. Levy, and R. M. Osgood Jr., "Laser-fabricated low-loss single-mode waveguiding devices in GaAs," *J. Lightwave Technol.*, p. 1610, 1992.

[18] M. Levy, L. Eldada, R. Scarmozzino, R. M. Osgood Jr., P. S. D. Lin, and F. Tong, "Fabrication of narrow-band channel-dropping filters," *Photon. Technol. Lett.*, p. 1378, 1992.

[19] L. Eldada, M. N. Ruberto, M. Levy, R. Scarmozzino, and R. M. Osgood Jr., "Rapid direct fabrication of active electrooptic modulators in GaAs," *J. Lightwave Technol.*, p. 1588, 1994.

[20] I. Ilic, R. Scarmozzino, R. M. Osgood Jr., J. T. Yardley, K. W. Beeson, and M. J. McFarland, "Modeling multimode-input star couplers in polymers," *J. Lightwave Technol.*, p. 996, 1994.

[21] ——, "Photopatterned polymer multimode 8x8 star couplers: Comparative design methodologies and device measurements," *IEICE Trans. Commun.*, 1997.

[22] M. C. Shih, M. Hu, M. B. Freiler, M. Levy, R. Scarmozzino, R. M. Osgood Jr., I. W. Tao, and W. I. Wang, "Fabrication of an InGaAs SQW Circular Ring Laser By Direct Laser Patterning," *Appl. Phys. Lett.*, p. 2608, 1995.

[23] L. Eldada, R. Scarmozzino, R. M. Osgood Jr., D. C. Scott, Y. Chang, and H. R. Fetterman, "Laser-fabricated delay lines in GaAs for optically-steered phased-array radar," *J. Lightwave Technol.*, p. 2034, 1995.

[24] M. H. Hu, Z. Huang, K. L. Hall, R. Scarmozzino, and R. M. Osgood Jr., "An integrated two-stage cascaded Mach–Zehnder device in GaAs," *J. Lightwave Technol.*, vol. 16, pp. 1447–1455, 1998.

[25] M. Hu, R. Scarmozzino, M. Levy, and R. M. Osgood Jr., "A low-loss and compact waveguide y-branch using refractive index tapering," *Photon. Technol. Lett.*, vol. 9, pp. 203–205, 1997.

[26] R. Scarmozzino, R. M. Osgood Jr., L. Eldada, J. T. Yardley, Y. Liu, J. Bristow, J. Stack, J. Rowlette, and Y. S. Liu, "Design and fabrication of passive optical components for multimode parallel optical links," in *Proc. SPIE Photonic West Meeting*, vol. 3005, San Jose, CA, Feb. 1997, p. 257.

[27] M. Hu, J. Z. Huang, R. Scarmozzino, M. Levy, and R. M. Osgood Jr., "Tunable Mach–Zehnder polarization splitter using height-tapered y-branches," *Photon. Technol. Lett.*, vol. 9, pp. 773–775, 1997.

[28] D. S. Levy, Y. M. Li, R. Scarmozzino, and R. M. Osgood Jr., "A multimode interference-based variable power splitter in GaAs–AlGaAs," *Photon. Technol. Lett.*, vol. 9, pp. 1373–1375, 1997.

[29] D. S. Levy, R. Scarmozzino, Y. M. Li, and R. M. Osgood Jr., "A new design for ultracompact multimode interference-based 2x2 couplers," *Photon. Technol. Lett.*, vol. 10, pp. 96–98, 1998.

[30] J. Z. Huang, M. H. Hu, J. Fujita, R. Scarmozzino, and R. M. Osgood Jr., "High-performance metal-clad multimode interference devices for low-index-contrast material systems," *Photon. Technol. Lett.*, vol. 10, pp. 561–563, 1998.

[31] J. Z. Huang, R. Scarmozzino, and R. M. Osgood Jr., "A new design approach to large input/output-number multimode interference couplers and its application to low-crosstalk WDM routers," *Photon. Technol. Lett.*, vol. 10, pp. 1292–1294, 1998.

[32] D. S. Levy, K. H. Park, R. Scarmozzino, R. M. Osgood Jr., C. Dries, P. Studenkov, and S. Forrest, "Fabrication of ultracompact 3-dB 2x2 MMI power splitters," *Photon. Technol. Lett.*, vol. 11, pp. 1009–1011, 1999.

[33] T. A. Ramadan, R. Scarmozzino, and R. M. Osgood Jr., "Adiabatic couplers: Design rules and optimization," *J. Lightwave Technol.*, vol. 16, pp. 277–283, 1998.

[34] J. Fujita, M. Levy, R. Scarmozzino, R. M. Osgood Jr., L. Eldada, and J. T. Yardley, "Integrated multistack waveguide polarizer," *Photon. Technol. Lett.*, vol. 10, pp. 93–95, 1998.

[35] J. Z. Huang, R. Scarmozzino, G. Nagy, M. J. Steel , and R. M. Osgood Jr., , submitted for publication.

[36] D. Yevick and B. Hermansson, "Efficient beam propagation techniques," *J. Quantum Electron.*, vol. 26, pp. 109–112, 1990.

[37] Y. Chung and N. Dagli, "An assessment of finite difference beam propagation method," *J. Quantum Electron.*, vol. 26, pp. 1335–1339, 1990.

[38] R. Scarmozzino and R. M. Osgood Jr., "Comparison of finite-difference and Fourier-transform solutions of the parabolic wave equation with emphasis on integrated-optics applications," *J. Opt. Soc. Amer. A*, vol. 8, p. 724, 1991.

[39] G. R. Hadley, "Transparent boundary condition for the beam propagation method," *Opt. Lett.*, vol. 28, p. 624, 1992.

[40] C. Vassalo and F. Collino, "Highly efficient absorbing boundary condition for the beam propagation method," *J. Lightwave Technol.*, vol. 14, pp. 1570–1577, 1996.

[41] W. P. Huang, C. L. Xu, W. Lui, and K. Yokoyama, "The perfectly matched layer (PML) boundary condition for the beam propagation method," *Photon. Technol. Lett.*, vol. 8, pp. 649–651, 1996.

[42] Y. P. Chiou and H. C. Chang, "Complementary operators method as the absorbing boundary condition for the beam propagation method," *Photon. Technol. Lett.*, vol. 8, pp. 976–979, 1998.

[43] W. H. Press, B. P. Flannery, S. A. Teuklsky, and W. T. Vetterling, *Numerical Recipes: The Art of Scientific Computing*. New York: Cambridge Univ. Press, 1986.

[44] R. Clauberg and P. Von Allmen, "Vectorial beam propagation method for integrated optics," *Electron. Lett.*, vol. 27, p. 654, 1991.

[45] W. P. Huang and C. L. Xu, "Simulation of three-dimensional optical waveguides by a full-vector beam propagation method," *J. Quantum Electron.*, vol. 29, p. 2639, 1993.

[46] D. Yevick and M. Glasner, "Analysis of forward wide-angle light propagation in semiconductor rib waveguides and integrated-optic structures," *Electron. Lett.*, vol. 25, pp. 1611–1613, 1989.

[47] G. R. Hadley, "Wide-angle beam propagation using Pade approximant operators," *Opt. Lett.*, vol. 17, p. 1426, 1992.

[48] H. J. W. M. Hoekstra, G. J. M. Krijnen, and P. V. Lambeck, "New formulations of the beam propagation method based on the slowly varying envelope approximation," *Opt. Commun.*, vol. 97, pp. 301–303, 1993.

[49] I. Ilic, R. Scarmozzino, and R. M. Osgood Jr., "Investigation of the Pade approximant-based wide-angle beam propagation method for accurate modeling of waveguiding circuits," *J. Lightwave Technol.*, vol. 14, pp. 2813–2822, 1996.

[50] P. Kaczmarski and P. E. Lagasse, "Bidirectional beam propagation method," *Electron. Lett.*, vol. 24, pp. 675–676, 1988.

[51] Y. Chung and N. Dagli, "Modeling of guided-wave optical components with efficient finite-difference beam propagation methods," in *Tech. Dig. IEEE AP-S Int. Symp.*, vol. 1, 1992, pp. 248–251.

[52] Y. Chiou and H. Chang, "Analysis of optical waveguide discontinuities using the Pade approximants," *Photon. Technol. Lett.*, vol. 9, pp. 964–966, 1997.

[53] H. Rao, R. Scarmozzino, and R. M. Osgood Jr., "A bidirectional beam propagation method for multiple dielectric interfaces," *Photon. Technol. Lett.*, vol. 11, pp. 830–832, 1999.

[54] C. L. Xu, W. P. Huang, J. Chrostowski, and S. K. Chaudhuri, "A full-vectorial beam propagation method for anisotropic waveguides," *J. Lightwave Technol.*, vol. 12, p. 1926, 1994.

[55] J. Yamauchi, J. Shibayama, and H. Nakano, "Modified finite-difference beam propagation method based on the generalized Douglas scheme for variable coefficients," *Photon. Technol. Lett.*, vol. 7, p. 661, 1995.

[56] G. R. Hadley, "Low-truncation-error finite difference equations for photonics simulation I: beam propagation," *J. Lightwave Technol.*, vol. 16, pp. 134–141, 1998.

[57] H. J. W. M. Hoekstra, G. J. M. Krijnen, and P. V. Lambeck, "Efficient interface conditions for the finite difference beam propagation method," *J. Lightwave Technol.*, vol. 10, pp. 1352–1355, 1992.
[58] J. Yamauchi, M. Sekiguchi, O. Uchiyama, J. Shibayama, and H. Nakano, "Modified finite-difference formula for the analysis of semivectorial modes in step-index optical waveguides," *Photon. Technol. Lett.*, vol. 9, pp. 961–963, 1997.
[59] M. D. Feit and J. A. Fleck, "Computation of mode properties in optical fiber waveguides by a propagating beam method," *Appl. Opt.*, vol. 19, p. 1154, 1980.
[60] D. Yevick and B. Hermansson, "New formulations of the matrix beam propagation method: Application to rib waveguides," *J. Quantum Electron.*, vol. 25, pp. 221–229, 1989.
[61] S. Jungling and J. C. Chen, "A study and optimization of eigenmode calculations using the imaginary-distance beam-propagation method," *J. Quantum Electron.*, vol. 30, p. 2098, 1994.
[62] D. Yevick and D. W. Bardyszewski, "Correspondence of variational finite-difference (relaxation) and imaginary-distance propagation methods for modal analysis," *Opt. Lett.*, vol. 17, pp. 329–330, 1992.
[63] G. R. Hadley and R. E. Smith, "Full-vector waveguide modeling using an iterative finite-difference method with transparent boundary conditions," *J. Quantum Electron.*, 1995.
[64] J. C. Chen and S. Jungling, "Computation of higher-order waveguide modes by the imaginary-distance beam propagation method," *Opt. Quantum Electron.*, vol. 26, pp. S199–S205, 1994.
[65] R. Pregla and W. Pascher, "The method of lines," in *Numerical Techniques for Microwave and Millimeter Wave Passive Structures*, T. Itoh, Ed. New York: Wiley, 1989, pp. 381–446.
[66] J. Gerdes and R. Pregla, "Beam-propagation algorithm based on the method of lines," *J. Opt. Soc. Amer. B*, vol. 8, no. 2, pp. 389–394, 1991.
[67] R. Pregla, "MoL-BPM method of lines based beam propagation method," in *Methods for Modeling and Simulation of Guided-Wave Optoelectronic Devices (PIER 11)*, W. P. Huang, Ed. Cambridge, MA: EMW Publishing, 1995, pp. 51–102.
[68] G. Guekos, *Photonic Devices for Telecommunications*. Berlin, Germany: Springer, 1999.
[69] U. Rogge and R. Pregla, "Method of lines for the analysis of dielectric waveguides," *J. Lightwave Technol.*, vol. 11, no. 12, pp. 2015–2020, 1993.
[70] R. Pregla, "The impedance/admittance transformation—An efficient concept for the analysis of optical waveguide structures," in *OSA Integr. Photo Research Tech. Dig.*, Santa Barbara, CA, July 1999, pp. 40–42.
[71] S. F. Helfert and R. Pregla, "Efficient analysis of periodic structures," *J. Lightwave Technol.*, vol. 16, pp. 1694–1702, Sept. 1998.
[72] I. A. Goncharenko, S. F. Helfert, and R. Pregla, "General analysis of fiber grating structures," *J. Opt. A*, vol. 1, pp. 25–31, 1999.
[73] A. S. Sudbø, "Improved formulation of the film mode matching method for mode field calculations in dielectric waveguides," *Pure Appl. Opt.*, vol. 3, pp. 381–388, 1994.
[74] J. Ctyrokÿ, S. Helfert, and R. Pregla, "Analysis of a deep waveguide Bragg grating," *Opt. Quantum Electron.*, vol. 30, pp. 343–358, 1998.
[75] U. Rogge and R. Pregla, "Method of lines for the analysis of strip-loaded optical waveguides," *J. Opt. Soc. Amer. B*, vol. 8, pp. 459–463, Feb. 1991.
[76] M. Bertolotti, M. Masciulli, and C. Sibilia, "MoL numerical analysis of nonlinear planar waveguide," *J. Lightwave Technol.*, vol. 12, pp. 784–789, 1994.
[77] R. Pregla, "A Generalized algorithm for analysis of planar multilayered anisotropic waveguide structures by the method of lines," *AEU*, vol. 52, no. 2, pp. 94–98, 1998.
[78] J. Gerdes, S. Helfert, and R. Pregla, "Three-dimensional vectorial eigenmode algorithm for nonparaxial propagation in reflecting optical waveguide structures," *Electron. Lett.*, vol. 31, no. 1, pp. 65–66, 1995.
[79] E. Ahlers and R. Pregla, "Modeling of y-branches with the MoL-BPM," in *OSA Integr. Photo Research Tech. Dig.*, San Francisco, CA, Feb. 1994, pp. 222–224.
[80] R. Pregla and E. Ahlers, "The method of lines for the analysis of discontinuities in optical waveguides," *Electron. Lett.*, vol. 29, no. 21, pp. 1845–1847, Oct. 1993.
[81] R. Pregla, J. Gerdes, E. Ahlers, and S. Helfert, "MoL-BPM algorithms for waveguide bends and vectorial fields," in *OSA Integr. Photo Research Tech. Dig.*, vol. 9, New Orleans, LA, 1992, pp. 32–33.
[82] R. Pregla and E. Ahlers, "Method of lines for analysis of arbitrarily curved waveguide bends," *Electron. Lett.*, vol. 30, no. 18, pp. 1478–1479, 1994.
[83] J. S. Gu, P. A. Besse, and H. Melchior, "Novel method for analysis of curved optical rib-waveguides," *Electron. Lett.*, vol. 25, pp. 278–280, 1989.
[84] ——, "Method of lines for the analysis of the propagation characteristics of curved optical rib waveguides," *IEEE J. Quantum Electron.*, vol. 27, no. 3, pp. 531–537, 1991.
[85] W. Pascher and R. Pregla, "Vectorial analysis of bends in optical strip waveguides by the method of lines," *Radio Sci.*, vol. 28, pp. 1229–1233, 1993.
[86] R. Pregla, "The method of lines for modeling of integrated optics structures," in *Latsis Symp. Computational Electromagnetics*, H. Baggenstos, Ed.. Zurich, 1995, pp. 216–229.
[87] S. Helfert, "Analysis of curved bends in arbitrary optical devices using cylindrical coordinates," *IEEE J. Quantum Electron.*, vol. 30, pp. 359–368, 1998.
[88] S. Helfert and R. Pregla, "Modeling of taper structures in cylindrical coordinates," in *Integr. Photo Research Tech. Dig.*, vol. 7, Dana Point, Feb. 1995, pp. 30–32.
[89] E. Ahlers, S. F. Helfert, and R. Pregla, "Modeling of VCSEL's by the method of lines," in *OSA Integr. Photo Research Tech. Dig.*, vol. 6, Boston, MA, 1996, pp. 340–343.
[90] O. Conradi, S. Helfert, and R. Pregla, "Modification of the finite difference scheme for efficient analysis of thin lossy metal layers in optical devices," *Opt. Quantum Electron.*, vol. 30, no. 14, pp. 369–373, 1998.
[91] S. F. Helfert and R. Pregla, "Modeling of thin dielectric layers in finite difference schemes," in *OSA Integr. Photo Research Tech. Dig.*, Santa Barbara, CA, July 1999, pp. 253–255.
[92] R. Pregla, "The method of lines for modeling of integrated optics structures," in *Proc. Latsis Symp. Computational Electromagnetics*, H. Baggenstos, Ed.. Zurich, 1995, pp. 216–229.
[93] K. S. Yee, "Numerical solution of initial boundary value problems involving Maxwell's equations in isotropic media," *IEEE Trans. Antennas Propagat.*, vol. AP-14, pp. 302–307, 1966.
[94] A. Taflov, *Computational Electrodynamics: The Finite Difference Time Domain Method*. Norwood, MA: Artech House, 1995.
[95] G. Strang, "On the construction and comparison of difference schemes," *SIAM J. Numer. Anal.*, vol. 5, pp. 506–517, 1968.
[96] J. S. Shang, "Characteristic based methods for the time-domain Maxwell equations," *IEEE Antennas Propagat. Mag.*, vol. 37, pp. 15–25, 1995.
[97] P. Colella and P. R. Woodward, "The piecewise parabolic method (PPM) for gas dynamical simulations," *J. Comp. Phys.*, vol. 54, pp. 174–201, 1984.
[98] P. R. Hayes, M. T. O'Keefe, and A. Gopinath, "Higher order compact time domain numerical simulation of optical waveguides," J. Opt. Quantum Electronics, to be published.
[99] G. R. Hadley, "Transparent boundary condition for the beam propagation method," *J. Quantum Electron.*, vol. 28, p. 363, 1992.
[100] G. R. Hadley, "Multistep method for wide-angle beam propagation," *Opt. Lett.*, vol. 17, p. 1743, 1992.

R. Scarmozzino (M'98) received the B.S. and M.S. degrees from the School of Engineering and Applied Science, Columbia University, New York, in 1982 and 1983 and the Ph.D. degree from the Graduate School of Arts and Sciences, Columbia University, in 1987, all in applied physics.

His graduate research was in the area of plasma physics and primarily consisted of an experimental and theoretical study of collisionless trapped particle instabilities. Subsequent to completing the Ph.D. degree, he joined the Columbia University Microelectronics Sciences Laboratories (MSL) and began research in a variety of laser-induced semiconductor processing techniques, developing novel techniques for etching, deposition, and doping of materials which include semiconductors (Si, GaAs, InP), metals (chiefly Al), and polymers. These techniques have been applied to various device fabrication problems, and several have been transferred to industrial collaborators for potential use in manufacturing. Since 1990, he has been involved in experimental and theoretical work on novel photonic devices. These efforts have led to the realization of several state-of-the-art photonic devices useful for communications and networking applications, and the first demonstration of several new techniques for prototyping photonic integrated circuits. In conjunction with the above mentioned experimental program in integrated optics, he has been active in developing numerical algorithms for the simulation of photonic devices and circuits. This work led to the development, in 1994, of BeamPROP, one of the first general purpose software tools for design of photonic devices. In parallel with his research at Columbia, Dr. Scarmozzino co-founded RSoft, Inc., a company specializing in development of computer-aided design (CAD) and simulation tools for photonic devices and systems. Currently, his primary position is Chief Scientist at RSoft, Inc.; he also continues to work closely with the research group of Prof. R. M. Osgood at the Columbia University Microelectronics Sciences Laboratory.

Dr. Scarmozzino has been a member of the American Physical Society, the Materials Research Society, the Electrochemical Society, the International Society for Optical Engineering, IEEE/LEOS, and the Sigma Xi Society.

A. Gopinath, photograph and biography not available at time of publication.

R. Pregla (M'76–SM'83–F'99) received the Dipl.-Ing. degree and the Dr.-Ing. degree in electrical engineering from the Technische Universität Braunschweig, Federal Republic of Germany, in 1963 and 1966, respectively.

From 1966 to 1969, he was a Research Assistant in the Department of Electrical Engineering of the Technische Universität Braunschweig (Institut für Hochfrequenztechnik), where he was engaged in investigations of microwave filters, group delay equalizers, and in electromagnetic field analysis. After the Habilitation, he was a Lecturer in high frequencies at the Technische Universität Braunschweig. Since 1973 he has held the position of Professor at the Ruhr-Universität Bochum, Germany, and since 1975, he has held the position of full Professor in Electrical Engineering at the FernUniversität (a university for distance study), Hagen, Germany. His fields of investigation include microwave and millimeter-wave integrated circuits, field theory, antennas and integrated optics and photonics. He is the inventor of the Method of Lines for applications in these fields. He has steadily improved this method and developed it into an efficient analysis and modeling tool. He has authored or co-authored around 200 papers in international journals and conference proceedings.

Dr. Pregla is a member of the IEEE TRANSACTIONS ON MICROWAVE THEORY AND TECHNIQUES Editorial Board and of the Technical Program Committee for the IEEE MTT-S International Microwave Symposium. In 1999 he was elected IEEE Fellow for his contributions to the analysis, modeling, and design of microwave and optical components.

S. Helfert was born in Marl, Germany. He received the Master's degree in electrical engineering (Dipl.-Ing.) from the Universität Dortmund in 1994.

Since 1994 he has been with the FernUniversität, Hagen, Germany, as a Research Assistant. His main research interest is the analysis of integrated optical structures.

PROJET : ETUDE D'UNE JONCTION Y ASYMÉTRIQUE

1 Introduction

Ce projet vous propose d'étudier le comportement d'une jonction Y asymétrique dans le but de réaliser un coupleur démultiplexeur 980/1550.

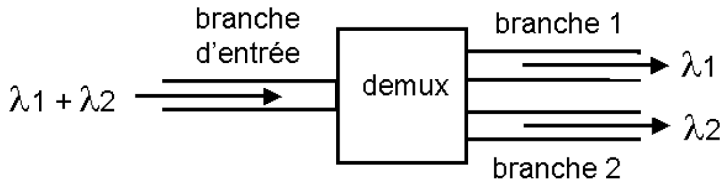

FIG. 1 – principe d'un démultiplexeur

La jonction Y asymétrique proposée comporte un bras de largeur plus petite et d'indice plus élevé. La figure 2 présente schématiquement le design envisagé.

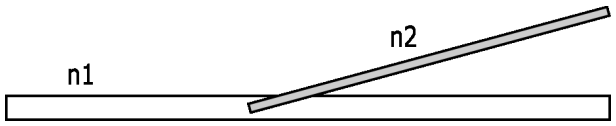

FIG. 2 – design de la jonction Y asymétrique

2 Contraintes générales

On utilisera les paramètres technologiques suivants :
. Indice du substrat : 1.51
. Différence d'indice : 7.10^{-3} pour le bras large et le bras d'accès
. Différence d'indice : 5.10^{-2} pour le bras étroit
. On souhaite effectuer la fonction de démultiplexage pour les longueurs d'ondes 980 et 1550 nm.

3 Etude du composant

Vous pourrez vous aider du plan de travail suivant :

. Trouver une largeur telle que le guide d'accès soit monomode aux deux longueurs d'ondes 980 et 1550 nm.
. Fixer l'angle θ à une valeur de 0,5 degrès. Utilisez un guide étroit courbé de manière à ce que les deux guides soient parallèles à l'axe optique en sortie.
. Faire varier la largeur du guide étroit. Mesurer alors l'isolation dans chaque bras (Isolation = 10.log (P1(λ1)/P2(λ1)) pour le bras 1)
. Tracer le diagramme puissance dans chaque bras en fonction de la longueur d'onde injectée. Déterminer alors la plage fréquentielle de fonctionnement à 1dB autour de 980 et 1550 nm.

PROJET : MULTIPLEXEUR EN LONGUEUR D'ONDE

1 Introduction

Le but de ce projet est d'étudier le fonctionnement d'un multiplexeur en longueur d'onde basé sur l'utilisation d'un coupleur directionnel, dont la structure est montrée figure 1. L'idée de base est d'utiliser l'interférence entre les deux modes de propagation (pair et impair) supportés par deux guides placés en interaction. Ce phénomène étant dépendant de la longueur d'onde, on peut l'exploiter pour réaliser une fonction de multiplexage/démultiplexage.

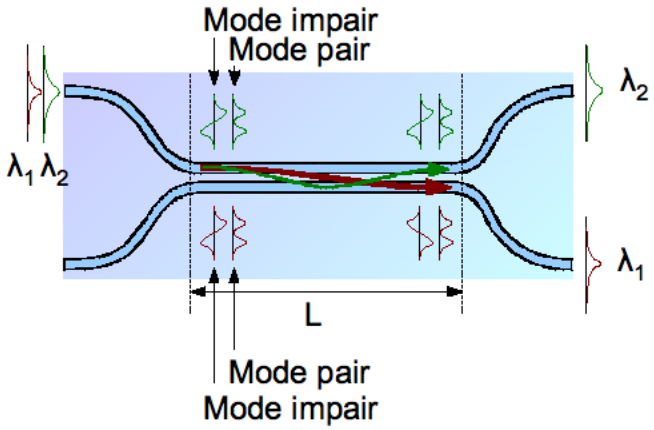

FIG. 1 – Structure de base d'un coupleur directionnel.

2 Contraintes générales

On utilisera les paramètres technologiques suivants :

- Longueurs d'onde de travail : 1,55 μm et 1,31 μm
- Indice du substrat : 1,5 (verre)
- Différence d'indice : 10^{-2}

3 Etude des guides

- Dimensionner les guides d'onde utilisées dans la structure pour qu'ils soient monomodes aux deux longueurs d'onde utilisées dans le système.

– Choisir une distance optimal entre les deux guides d'onde en interaction, afin d'optimiser la taille du dispositif.
– Mesurer alors l'isolation dans chaque bras aux longueurs d'onde nominales de fonctionnement (Isolation = 10.log (P1(λ1)/P2(λ1)) pour le bras 1)
– Tracer le diagramme puissance dans chaque bras en fonction de la longueur d'onde injectée. Déterminer alors la plage fréquentielle de fonctionnement à 1dB autour de 1310 nm et 1550 nm.

PROJET : ETUDE D'UN FILTRE COURTE LONGUEURS D'ONDES

1 Introduction

Ce projet vous propose d'étudier la variation fréquentielle du couplage d'un guide droit avec un guide plan. Le but est de réaliser un filtre frequentiel : laisser passer les courtes longueurs d'onde et faire fuir les hautes longueurs d'ondes. Ce filtre est basé sur la variation de l'étalement d'un mode guidé avec la longueur d'onde. La zone à fuite doit être très large devant la longueur d'onde (au moins 100 microns).

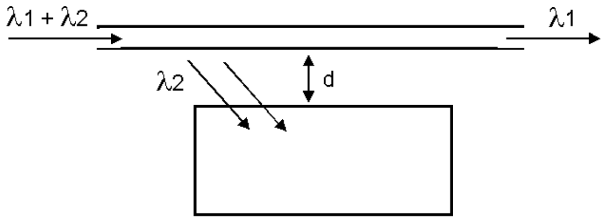

FIG. 1 – principe du filtre

La caractéristique principale attendue de ce type de composant est l'isolation. Celle-ci est donnée par :

$$I = 10 * log \frac{P(\lambda 1)}{P(\lambda 2)}$$

où $P(\lambda 1)$ et $P(\lambda 1)$ sont les puissances respectivement à la longueur d'onde $\lambda 1$ et $\lambda 2$ présentes à la sortie du guide droit. L'optimisation du composant consistera donc à faire fuir le maximum de puissance à $\lambda 2$ tout en conservant le maximum de puissance à $\lambda 1$ confinée dans le guide

2 Contraintes générales

On utilisera les paramètres technologiques suivants :
. Longueur d'onde à démultiplexer : 0.98 μm et 1.55 μm (utilisé dans les amplificateurs tout optique dopés Erbium)
. Indice du substrat : 1.51
. Différence d'indice : 7.10^{-3}(échange Sodium - Potassium) ou 8.10^{-2}(échange Sodium - Argent)
. taille maximale du dispositif : 5 cm.

3 Etude du composant

Vous pourrez vous aider du plan de travail suivant :

. Etude le la plage en largeur pour laquelle le guide d'amenée est monomode à 0.98 et 1.55 μm.
. Effet de la distance d entre le guide et la zone planaire.
. Effet de la différence d'indice dans les zones échangées.
. Optimisation du filtre : maximiser l'isolation du composant. Quelle est l'effet de la longueur du composant ?
Question subsidiaire :
. Etude de la récupération du signal à $\lambda 2$ dans un guide situé sous la zone planaire.

PROJET : ETUDE D'UN GUIDE SEGMENTE

Le but de ce projet est d'analyser l'équivalence entre un guide d'onde traditionnel et un guide segmenté. Ce dernier représente une possibilité de simuler un guide continu avec un contraste d'indice (différence d'indice de réfraction entre cœur et substrat) en réalisant une segmentation du cœur. Pour éviter un comportement résonnant (réseau de Bragg), la période de segmentation est choisie longue devant la longueur d'onde guidée.

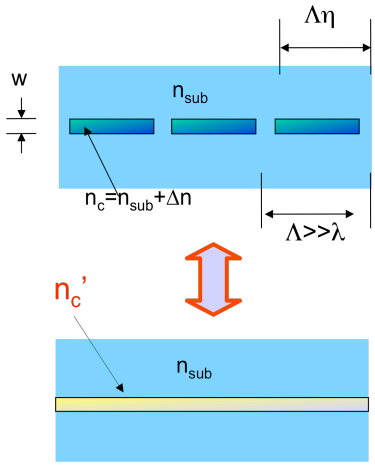

En pratique, une donnée technologique (contraste d'indice) devient contrôlable par un paramètre géométrique (masque de photolithographie). Si d'un côté la segmentation est efficace pour atteindre ce but, de l'autre les pertes introduites doivent être maîtrisées.

1 Contraintes générales

On utilisera les paramètres technologiques suivants :

- Longueur d'onde de travail 1,55 µm.
- Indice du substrat : 1,5 (verre)
- Différence d'indice : 3 x 10^{-2}

2 Etude du composant

Une stratégie de dimensionnement peut être la suivante :

- dimensionner un guide d'onde continu monomode à la longueur d'onde de travail
- segmenter le cœur (un script vous sera utile) et choisir une valeur Λ, de la période de segmentation, afin de contenir les pertes à 1 dB/cm.
- faire varier le rapport cyclique η et observer le comportement des pertes. Si le comportement est insatisfaisant, éventuellement revenir à l'étape précédente
- choisir une structure permettant de comparer les caractéristiques de propagation de deux guides. Un guide sera segmenté et le deuxième sera un guide continu de référence. Conclure sur l'efficacité de l'équivalence.

PROJET : COUPLEURS MMI

Le but de ce projet est de se familiariser avec les composants à base de section multimode ou MultiMode Interferometer(MMI). Dans ce but, vous étudierez le plus simple des composants MMI : le coupleur 2 vers 2.

FIG. 1 – Coupleur MMI 2 vers 2

1 Contraintes générales

On utilisera les paramètres technologiques suivants :
. Longueur d'onde de travail : 1.55 μm
. Indice du substrat : 1,5
. Différence d'indice : 10^{-2}

2 Coupleur 2 vers 2

L'étude du coupleur MMI 2→2 est destinée à une compréhension générale des phénomènes intervenant dans un coupleur à section multimode. La fonction de transfert d'un tel composant est la suivante : si l'on injecte les signaux A et B à l'entrée, on récupère (A+B)/2 sur chacune des sorties.
Votre travail est de minimiser les pertes du coupleur. Pour cela, vous pouvez vous aider de la description des composants de type MMI trouvée dans la littérature, ainsi que du plan de travail suivant :

. déterminer la largeur de la section multimode de sorte qu'elle supporte entre 7 et 9 modes guidés. Choisir une valeur sera conservée pour toute la suite.
. déterminer la taille des guides d'amenée pour que l'injection soit monomode. Choisir une valeur (plutôt un guide large) fixée pour toute la suite
. prenez la position des guides vis à vis de la section multimode suivante : $w/3$ et $2w/3$.
. déterminer la longueur maximale des guides d'entrée pour qu'il ne soient pas couplés.
. déterminer la longueur du MMI qui permet d'obtenir les images souhaitées des champs des guides d'entrée.
. ajouter les guides de sortie et vérifier que la fonction coupleur est bien remplie.
. évaluer les caractéristiques du coupleur : uniformité et pertes.

3 Bonus

. Recherchez une position des guides permettant un meilleur couplage avec les modes de la section multimode (n'hésitez pas a faire une recherche biblio !).
. Optimisez la taille des guides d'amenée, en conservant la position optimale trouvée précédemment.
. Analysez la stabilité aux paramètres technologiques et à la longueur d'onde.

PROJET : CAPTEUR MACH ZEHNDER

Le but de ce projet est de prendre en main une technique interférométrique utilisée pour réaliser des capteurs chimiques intégrés. La structure de base est montrée figure 1. Les deux bras de l'interféromètre sont de longueur identique, mais un est recouvert par un polymère dont l'indice de réfraction varie en fonction de la concentration d'un gaz. La différence de chemin optique entre les deux bras dépend donc de la concentration du gaz et peut donner lieu à des interférences constructives ou destructives à la sortie du dispositif.

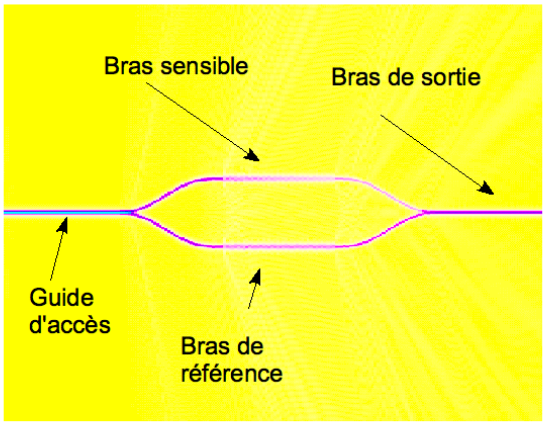

FIG. 1 – Structure de base d'un interféromètre de Mach-Zehnder.

1 Contraintes générales

On utilisera les paramètres technologiques suivants :

- Longueur d'onde de travail : 1,55 μm
- Indice du substrat : 1,5 (verre)
- Différence d'indice : 10^{-2}

2 Jonctions Y

La première jonction Y symétrique utilisée dans la structure est utilisée en tant que diviseur de puissance. Votre travail consiste d'abord à étudier cette fonction :

– dimensionnez les guides d'entrée et de sortie du système pour qu'ils supportent seulement le mode fondamental de propagation.
– analysez les pertes globales de la structure par rapport à l'angle de branchement. Rappelez vous que minimiser l'espace occupé réduit les coûts de fabrication.
– quelle est la relation de phase entre les champs qui se propagent dans les deux guides à la fin de la jonction Y ?

La deuxième jonction Y est utilisée en tant que recombineur. Nous allons considérer une structure parfaitement symétrique a celle utilisée en tant que diviseur de puissance.

– que se passe-t-il si les deux guides d'accès sont excités en phase ?
– et s'il y a un déphasage de 180° ?

3 Zone sensible

Un bras de l'interférométre est recouvert par un polymère qui a la proprieté de modifier son indice de réfraction de 1,44 à 1,46 avec loi linéaire en présence d'un changement de concentration de 0 à 10% en volume dans l'air d'une espèce chimique particulière. L'autre bras de l'interféromètre est recouvert par un superstrat inerte dont l'indice de réfraction est fixé à 1,44.

– Déterminer la longueur optimale du système, afin d'optimiser sa sensibilité.
– Analyser la stabilité aux paramètres technologiques et à la longueur d'onde.